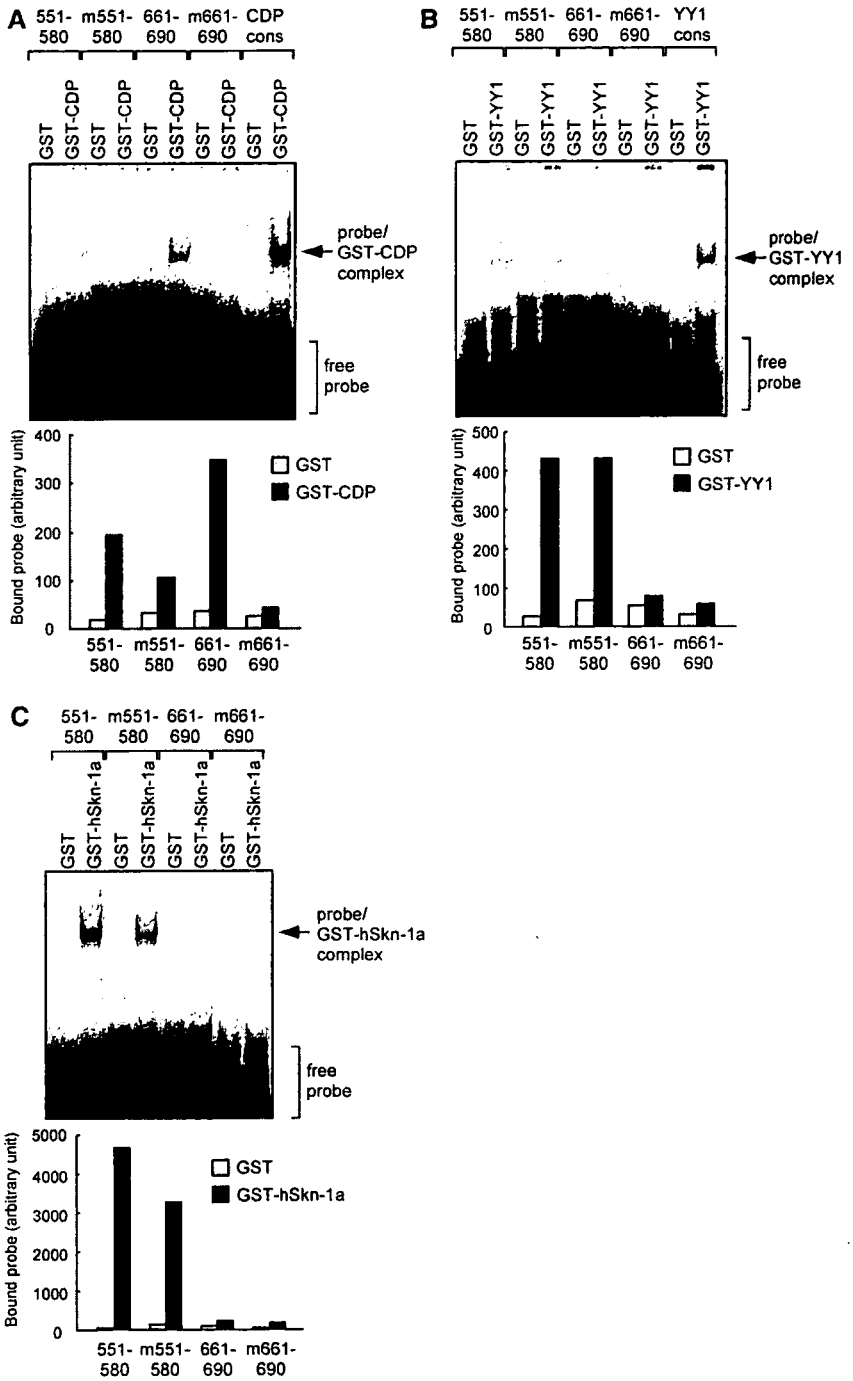

Fig. 4 The EMSA **(A)** EMSA detecting the complex of GST-CDP with [^{32}P]-labeled DNA probes with nucleotide sequences from nt 546 to 565 and from nt 666 to 685: The CDP DNA-binding domain was bacterially expressed as a fusion protein with GST and purified. DNA probes were synthesized and labeled with ^{32}P. 551–580 has nucleotide sequence from nt 551 to 580. The nucleotides from nt 546 to 565 in probe 551–580 were replaced with the mutant sequence (Fig. 2B) to produce m551–580. Similarly, 661–690 has nucleotide sequence from nt 661 to 669. The nucleotides from nt 666 to 685 in probe 661–669 were replaced with the mutant sequence to produce m661–690. The DNA-protein complex was electrophoresed on a 5% polyacrylamide gel and visualized by autoradiography. A DNA probe having a consensus CDP binding sequence was used as a positive control for EMSA (CDP cons). The level of bound probe was measured by a BAS-2500 (Fuji film co. Ltd., Tokyo, Japan) and presented below the autoradiogram. **(B)** EMSA detecting the complex of GST-YY1 with the [^{32}P]-labeled probes The YY1 DNA-binding domain was bacterially expressed as a fusion protein with GST and purified. The probes were described above. A DNA probe having a consensus YY1 binding sequence was used as a positive control (YY1 cons). The level of bound probe was presented below the autoradiogram. **(C)** EMSA detecting the complex of GST-hSkn-1a with the [^{32}P]-labeled probes. The bacterially expressed and purified GST-hSkn-1a was used in EMSA as shown in (A) and (B) in place of GST-CDP and GST-YY1. The level of bound probe was presented below

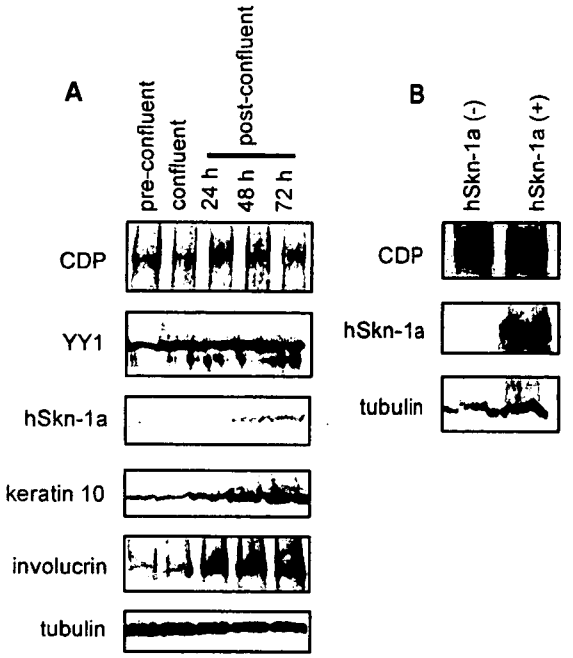

Fig. 5 Immunoblotting **(A)** HaCaT cells HaCaT cells from the 80% confluent culture and the fully confluent culture with the low-Ca-medium were collected as undifferentiated cells and confluent cells, respectively. The confluent cultures were further maintained with the high-Ca-medium. The cells were collected at 24 (correspond to the partially differentiated state in Fig. 2), 48, and 72 h after the medium replacement. The cells were lysed in the SDS-sample buffer and electrophoresed on SDS-polyacrylamide gel. The proteins were transferred to a nitrocellulose membrane electrically. The membrane was incubated with anti-CDP, anti-YY1, anti-Skn-1a, anti-keratin 10, anti-involucrin, or anti-alpha-tubulin. The membranes were then incubated with peroxidase-conjugated goat anti-rabbit or anti-mouse antibodies. **(B)** HeLa/hSkn-1a cells HeLa/hSkn-1a cells cultured with the growth medium with or without doxycycline (4 μg/ml) for 48 h were collected and lysed. The samples were processed as described above

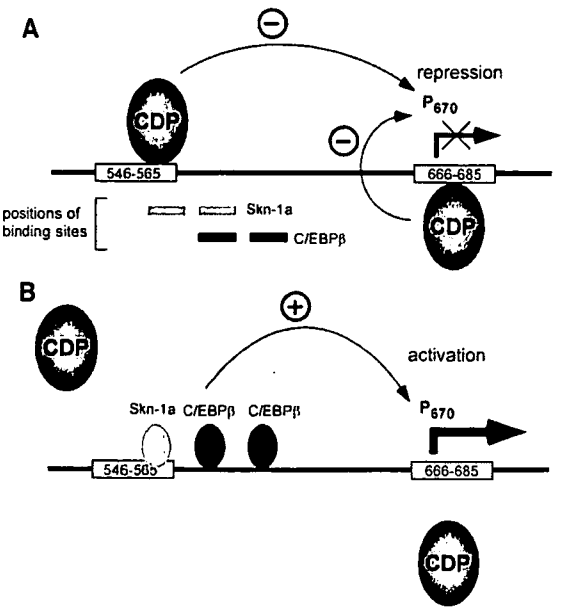

Fig. 6 A model of P_{670} regulation **(A)** Repression of transcription from P_{670} in the undifferentiated cells: CDP binds to the two sites in the P_{670} promoter region and strongly repress the transcription even in the presence of the activating factors, such as hSkn-1a and C/EBPβ, induced in the partially differentiated cells. **(B)** Activation of transcription from P_{670} in the differentiated cells: In the late phase of keratinocyte differentiation the affinity of CDP to the binding sites is reduced by a yet unknown mechanism and CDP comes off from the two sites. Then, the activating factors bind to the specific binding sites and induce efficient transcription from P_{670}

the binding of hSkn-1a to the promoter region. Therefore, transcription from pM (546–565) and pM (666–685), which escaped repression by CDP, were enhanced by hSkn-1a in the partially differentiated HaCaT and hSkn-1a-positive HeLa/hSkn-1a cells (Fig. 2).

CCAAT displacement protein family proteins, such as Cut in *Drosophila melanogaster* and Cux in mice, function in undifferentiated cells as a transcriptional repressor for genes that later become expressed in terminally differentiated cells [16]. CDP has been reported to repress gene expression by occupying binding sites for transcriptional activators [22, 23]. DNA-binding activity of CDP is down-regulated during B-cell and myeloid cell development [24, 25]. Expression of CDP in the kidney is inversely related with progression of cellular differentiation [26].

Recently it was reported that CDP recruits G9a histone lysine methyltransferase to cellular promoters to achieve repression of target genes [27]. Deacetylation of histones H3/H4 and lysine 9 methylation of histone H3 leads to a chromatin state highly repressive for transcription. Since the P_{670} region (between nt 519 and 679) is occupied by a positioned-nucleosome in the CaSki cell [28], which contains integrated copies of HPV16 DNA, the repressive histone modifications by CDP in the P_{670}-positioned nucleosome may contribute to strong suppression of P_{670} in undifferentiated keratinocytes.

Taken together, it is very likely that CDP directly binds to the two sites in the P_{670} promoter region and strongly represses P_{670} transcriptional activity in undifferentiated keratinocytes (Fig. 6). The transcription factors, such as hSkn-1a [13] and CEBPβ [15], capable of up-regulating transcription from P_{670} are expressed in the host cells in the early stage of differentiation. However, CDP-mediated repression may be predominant over the activators. Then, in the later stage of the host cell differentiation CDP may be released from the binding sites, as in the terminally

differentiating B-cells and myeloid cells [24, 25], and the transcription from P_{670} may be drastically enhanced to produce a large amount of capsid protein.

It has been shown that the HPV6 promoters are negatively regulated by CDP [18]. Transient reporter expressions from the HPV6b three promoters, P_{90}, P_{270}, and P_{680}, in primary human keratinocytes are repressed by co-transfection with expression plasmid for CDP. The binding motif of CDP exists in the late promoter regions of HPV18, 31, 45, 52, and 58. Thus, the CDP-mediated repression of HPV promoters is likely to be a common molecular mechanism to support the HPV life cycle tightly associated with the differentiation of the host cells. To obtain further information on the regulation of transcription from P_{670} it is necessary to establish a system for the efficient productive infection of HPV in the terminally differentiated cultured cells.

Acknowledgments We thank Dr. Ellis Neufeld and Dr. Alain Nepveu for kind supply of the human CDP, cDNA, and the anti-CDP antiserum, respectively. This work was supported by a grant-in-aid from the Ministry of Health, Labour and Welfare for the Third-Term Comprehensive Control Research for Cancer and for the Research on Human Genome and Tissue Engineering.

References

1. H. Zur Hausen, Biochem. Biopyys. Acta **1288**, F55 (1996)
2. M.S. Longworth, L.A. Laimins, Microbiol. Mol. Biol. Rev. **68**, 362 (2004)
3. H. Zur Hausen, J. Natl. Cancer Inst. **92**, 690 (2000)
4. F. Fehrmann, L.A. Laimins, Oncogene **22**, 5201 (2003)
5. K. Grassmann, B. Rapp, H. Maschek, K.U. Petry, T. Iftner, J. Virol. **70**, 2339 (1996)
6. M. Hummel, J.B. Hudson, L.A. Laimins, J. Virol. **66**, 6070 (1992)
7. D.J. Klumpp, L.A. Laimins, Virology **257**, 239 (1999)
8. M.A. Ozbun, C. Meyers, J. Virol. **71**, 5161 (1997)
9. M.N. Ruesch, F. Stubenrauch, L.A. Laimins, J. Virol. **72**, 5016 (1998)
10. A.K. Ryan, M.G. Rosenfeld, Genes Dev. **11**, 1207 (1997)
11. B. Andersen, A. Hariri, M.R. Pittelkow, M.G. Rosenfeld, J. Biol. Chem. **272**, 15905 (1997)
12. J. Hildesheim, R.A. Foster, M.E. Chamberlin, J.C. Vogel, J. Biol. Chem. **274**, 26399 (1999)
13. I. Kukimoto, T. Kanda, J. Virol. **75**, 9302 (2001)
14. K. Yukawa, K. Butz, T. Yasui, H. Kikutani, F. Hoppe-Seyler, J. Virol. **70**, 10 (1996)
15. I. Kukimoto, T. Takeuchi, T. Kanda, Virology **346**, 98 (2006)
16. A. Nepveu, Gene **270**, 1 (2001)
17. M.J. O'connor, W. Stuenkel, C.H. Koh, H. Zimmermann, H. Bernard, J. Virol. **74**, 401 (2000)
18. W. Ai, E. Toussaint, A. Roman, J. Virol. **73**, 4220 (1999)
19. Y. Enomoto, K. Enomoto, T. Kitamura, T. Kanda, Oncogene **23**, 5014 (2004)
20. E.J. Neufeld, D.G. Skalnik, P.M.-J. Lievens, S.H. Orkin, Nat. Genet. **1**, 50 (1992)
21. B.K. Steele, C. Meyers, M.A. Ozbun, Anal. Biochem. **307**, 341 (2002)
22. W. Luo, D.G. Skalnik, J. Biol. Chem. **271**, 18203 (1996)
23. N.S. Moon, G. Berube, A. Nepveu, J. Biol. Chem. **275**, 31325 (2000)
24. P.M. Lievens, J.J. Donady, C. Tufarelli, E.J. Neufeld, J. Biol. Chem. **270**, 12745 (1995)
25. Z. Wang, A. Goldstein, R.T. Zong, D. Lin, E.J. Neufeld, R.H. Scheuermann, P.W. Tucker, Mol. Cell. Biol. **19**, 284 (1999)
26. G.B. Vanden Heuvel, R. Bodmer, K.R. McConnell, G.T. Nagami, P. Igarashi, Kidney Int. **50**, 453 (1996)
27. H. Nishio, M.J. Waish, Proc. Natl. Acad. Sci. USA **101**, 11257 (2004)
28. W. Stuenkel, H. Bernard, J. Virol. **73**, 1918 (1999)

Journal of Medical Virology 80:841–846 (2008)

Modification of Human Papillomavirus-Like Particle Vaccine by Insertion of the Cross-Reactive L2-Epitopes

Kazunari Kondo,[1,2] Hiroyuki Ochi,[1,2] Tamae Matsumoto,[1] Hiroyuki Yoshikawa,[2] and Tadahito Kanda[1]*

[1]*Center for Pathogen Genomics, National Institute of Infectious Diseases, Shinjuku-ku, Tokyo, Japan*
[2]*Department of Obstetrics and Gynecology, University of Tsukuba, Tsukuba-shi, Ibaraki, Japan*

Infection with human papillomavirus 16 (HPV16), which is one of the 15 types of HPV causally associated with cervical cancer and accounts for 50% of the cases, can be prevented in a type-specific manner by an HPV16 virus-like particle (VLP) vaccine comprised of particles of the L1 protein alone. We attempted to modify the VLP vaccine by inserting the HPV16 L2-peptides including cross-neutralization epitopes into the L1 polypeptide. The chimeric L1 had, between L1 amino acids (aa) 430 and 433, the L2 sequence of aa 18–38, 56–75, or 96–115 (with the replacements of S at aa 101 and T at aa 112 with L and S, respectively). The three chimeric L1s were each expressed from the recombinant baculovirus in insect Sf9 cells, and the resultant VLPs were characterized. The chimeric VLPs were shown to present the L2-peptides on their surface. By immunizing rabbits with the VLPs, it was shown that they retained capability to induce the antibody neutralizing HPV16 and acquired capability to elicit antibodies cross-neutralizing the infectious HPV18, 31, 52, and 58 pseudovirions. Although the cross-neutralizing titers were lower than the type-specific neutralizing titer, the results suggest that the chimeric VLPs have potential to serve as a vaccine candidate for a broad spectrum of high-risk HPVs. ***J. Med. Virol. 80:841–846, 2008.*** © 2008 Wiley-Liss, Inc.

KEY WORDS: HPV; L2-epitope; chimeric VLP

INTRODUCTION

Cervical cancer, the second most frequent gynecological malignancy in the world [Ferlay et al., 2004], is caused by genital infection with the high-risk human papillomaviruses (HPVs; types of 16, 18, 31, 33, 35, 39, 45, 51, 52, 56, 58, 59, 66, 68, and 73) [Munoz et al., 2004]. Therefore, a vaccine that prevents the persistent HPV infection could reduce the incidence of the cancer. The distribution of high-risk HPVs in humans slightly varies from region to region; HPV16 accounts for about 50% of the cases worldwide [Munoz et al., 2004; Clifford et al., 2006].

HPV16 is a nonenveloped virus having an 8-kb double-stranded circular genomic DNA encapsidated in an icosahedral capsid composed of 360 molecules of major capsid protein L1 (composed of 505 amino acids [aa]) and 12 molecules of minor capsid protein L2 (473 aa) [Trus et al., 1997]. Although cell cultures supporting efficient HPV replication are not available, the expression of L1 either alone or together with L2 in surrogate systems results in the spontaneous formation of particles without viral DNA, the virus-like particle (VLP) or the L1/L2-capsid, respectively [Kirnbauer et al., 1993; Volpers et al., 1994]. Expression of L1 and L2 in cells harboring episomal copies of an expression plasmid results in packaging of the episomal DNA into the L1/L2-capsids to produce infectious pseudovirions [Buck et al., 2004]. Although it is not clear whether the pseudovirions are assembled in the same way as the authentic HPV virion, the pseudovirions are used as a surrogate virus to detect neutralizing activity of anti-HPV antibodies [Pastrana et al., 2004].

The VLPs are highly immunogenic in animals [Kirnbauer et al., 1992] and humans [Koutsky et al., 2004] and induce a type-specific neutralizing antibody [Giroglou et al., 2001]. The prophylactic vaccines using VLPs of HPV6, 11, 16, and 18 as antigens have been developed. The vaccines successfully induced type-specific neutralizing antibodies in recipients in the large-scale clinical trials [Villa et al., 2005; Harper et al., 2006]. Although the preventive effect of the vaccine appears to be promising, one of the remaining

Grant sponsor: Ministry of Health, Labour and Welfare.

*Correspondence to: Dr. Tadahito Kanda, 1-23-1 Toyama, Shinjuku-ku, Tokyo 162-8640, Japan. E-mail: kanda@nih.go.jp

Accepted 20 December 2007
DOI 10.1002/jmv.21124
Published online in Wiley InterScience (www.interscience.wiley.com)

problems to be addressed is how to prevent infection with other high-risk HPVs.

HPV16 L2 N-terminal region, approximately from aa position 18–144, is displayed on the surface of the L1/L2-capsid and the antibody capable of binding to the L2-surface region abrogates infectivity of HPV pseudovirions [Kondo et al., 2007]. Rabbit antisera induced by synthetic peptides with sequences of HPV16 L2 aa 18–38, aa 56–75, aa 61–75, aa 64–81, or aa 96–115 neutralize the HPV16 pseudovirions and cross-neutralize the pseudovirions of one or more of HPV18, 31, and 58, indicating that these antigen peptides contain cross-neutralization L2-epitopes [Kondo et al., 2007].

Several animal experiments have indicated that L2-vaccines, as compared with the L1 VLP vaccine, induce in immunized animals a low level of neutralizing antibody against the infectious pseudovirions, but that they efficiently protect the animals against papillomavirus challenge. Vaccination of rabbits with a synthetic peptide with an aa sequence of L2 aa 94–112 or 107–122 of cottontail rabbit papillomavirus (CRPV) induced neutralizing antibody with titers ranging from 1:5 to 1:10 and protected the rabbits from CRPV challenge [Embers et al., 2002]. Vaccination of calves with a bacterially produced peptide with L2 aa 11–200 of bovine papillomavirus type 4 (BPV4) induced neutralizing antibody (with a titer of 1:5) and protected the calves against challenge with BPV4 [Gaukroger et al., 1996]. Vaccination of rabbits with a bacterially produced peptide having HPV16 L2 aa 11–200 was recently reported to efficiently cross-protect the rabbits against challenge with CRPV although titers of the cross-neutralizing antibody ranged from an undetectable level (1:<15) to 1:256 [Gambhira et al., 2007]. The neutralizing titers of the anti-L2 antisera are apparently much lower than those of anti-L1 antisera immunized with L1 VLP and assayed by the pseudovirion method (ranging from 1:10,000 to 1:100,000) [Pastrana et al., 2004; Gambhira et al., 2007]. Thus, it seems that the L2 vaccines that induce a relatively low neutralizing titer against infectious pseudovirions are capable of effectively protecting animals against papillomavirus infection [Gambhira et al., 2007].

In this study we modify a HPV16 VLP vaccine by inserting the peptides containing the cross-neutralizing L2-epitopes. It seems an attractive idea to add the cross-neutralization L2-epitopes to the current VLP vaccine, whose safety has been well established. The chimeric VLPs elicited in rabbits the antibody that can cross-bind to and cross-neutralize multiple high-risk HPVs.

MATERIALS AND METHODS

Preparation of Capsids

We inserted the following DNA segment encoding LYKTCKQAGTCPPDIIPKVEG (corresponding to HPV16 L2 aa 18–38), GGLGIGTGSGTGGRTGYIPL (aa 56–75), or DPVGPLDPSIVSLVEESSFI (aa 96–115 with replacement S at aa 101 and T at aa 112 with L and S, respectively) into the HPV16 L1 gene between aa 430 and aa 433 by a PCR-based strategy. The resultant DNA fragments were used to produce the recombinant baculoviruses capable of expressing the chimeric L1s with the Bac-to-Bac baculovirus expression system (Invitrogen Corp., Carlsbad, CA).

The recombinant baculovirus was inoculated to Sf9 cells (5 flasks of 175 cm^2 culture) and incubated for 72 hr at 27°C. The cells were collected and suspended in 5 ml of PBS containing 0.5% NP-40. After incubation for 10 min at room temperature (RT), the cells were centrifuged at 10,000*g* at 4°C for 15 min to precipitate nuclei. The nuclei were suspended in PBS containing CsCl (1.28 g/ml) and lysed with brief sonication (Sonifier250, Branson, Danbury, CT). The solution was centrifuged at 34,000 rpm for 20 hr at 20°C in an SW50.1 rotor (BECKMAN COULTER, Inc., Fullrerion, CA). The fractions around a buoyant density of 1.28 g/ml were pooled and dialyzed against PBS supplemented with 0.5 M NaCl at 4°C to remove CsCl. Then, the solution was layered on the top of a discontinuous sucrose-density gradient (5% and 60%) in PBS and centrifuged at 31,000 rpm for 2 hr at 4°C in an SW50.1 rotor. The particles between 5% and 60% sucrose layers were collected and dialyzed against PBS supplemented with 0.5 M NaCl at 4°C to obtain purified VLPs.

Electron Microscopy

The purified VLPs were allowed to settle on carbon-coated copper grids and stained with 4% uranylacetate. The grids were examined in a HITACHI model H-7600 transmission electron microscope and photographed at an instrumental magnification of 200,000×.

ELISA

Fifty microliters of VLPs (0.1 mg/ml in PBS) or 50 μl of the peptides (1 mg/ml in H_2O) synthesized by Fmoc method by SCRUM, Inc. (Tokyo, Japan) was added to each well of an ELISA plate (Thermo Labsystems, Franklin, MA) and incubated for 14–16 hr at 4°C. Then the wells were blocked with 5% skim milk in PBS containing 0.1% Tween-20 (Blocking buffer) for 2 hr at 37°C. After washings with PBS containing 0.05% Tween-20 and 0.05% NP-40, the serum samples diluted at 1:500 for peptide ELISA, 1:2,000 for VLP ELISA with Blocking buffer were added to wells and incubated for 1 hr at RT. The horseradish peroxidase-conjugated anti-rabbit IgG goat serum (SC-2030, Santa Cruz Biotechnology, Inc., Santa Cruz, CA) was diluted at 1:2,000 with Blocking buffer and was added to the wells. A mixture of 0.01% H_2O_2 and *o*-phenylenediamine (2 mg/ml) in 0.1M citrate buffer (pH4.7) was added to the wells and the absorbency at 450 nm was measured.

Immunization of Rabbits With Chimeric VLPs

Japanese white rabbits [2.3–3.0 kg of weight, 2 animals for Ch18/38 and Ch96/115(101L, 112S) VLPs and 4 animals for Ch56/75 VLP] were subcutaneously injected with the chimeric VLPs mixed with

TiterMaxGold (TiterMax USA, Inc., Norcross, GA) or HPV16VLP mixed with Freund's complete adjuvant by SCRUM, Inc. Immunization was repeated four times at 2 week's interval and serum was obtained at 1 week after the third immunization (first drawing, 5 ml) and at 1 week after the last immunization (second drawing). Except for anti-Ch96/115(101L, 112S)#2, the antisera obtained by the second drawing were used for the assays. Anti-Ch96/115(101L, 112S)#2 was antiserum obtained by the first drawing because the rabbit died prior to the second drawing. The antisera were filtered (Steradisc25, KURABO, Inc., Osaka, Japan) before use for the assays in this study.

Preparation of Pseudovirions and Neutralization Test

Five plasmids (pYSEAP expressing SEAP, p16L1h expressing HPV16 L1, p16L2h expressing HPV16 L2, peL1fB expressing HPV18 L1, and peL2bhb expressing HPV18 L2) were gifts from J. T. Schiller. Four plasmids (p31L1h expressing HPV31 L1, p31L2h expressing HPV31 L2, p58L1h expressing HPV58 L1, and p58L2h expressing HPV58 L2) were constructed previously [Kondo et al., 2007], and two plasmids (p52L1h expressing HPV52 L1 and p52L2h expressing HPV52 L2) were similarly constructed in this study.

293FT cells (Invitrogen Corp.), which had been seeded in a 10 cm culture dish (1×10^7 cells) at 16 hr before the transfection, were transfected with a mixture of an L1-plasmid (13.5 μg), an L2-plasmid (3 μg), and pYSEAP (13.5 μg) by using Fugene HD (Rosch Diagnostics GmbH, Mannheim, Germany). Fifty hours later the pseudovirions were extracted and purified from the cells as described previously [Kondo et al., 2007].

The neutralization test was carried out as described previously [Kondo et al., 2007] with the following minor modification; the mixture of the diluted serum and the pseudovirions was inoculated to 293FT cells, which had been seeded in a well of a 96-well plate (1×10^4 cells) at 16 hr before the inoculation. The neutralization titer was presented as the reciprocal of maximum dilution of serum that reduced the SEAP level to half of the sample not treated with serum.

RESULTS

Production of Chimeric VLPs Containing the L2-Epitopes

Figure 1A shows three chimeric L1s produced by insertion of the peptides containing the L2-epitopes. The DNA fragments encoding Ch18/38L1, Ch56/75L1, and Ch96/115(101L, 112S)L1 were newly constructed by inserting the DNA segments encoding aa positions 18–38, 56–75, and 96–115 (with the replacements of S at aa 101 and T at aa 112 with L and S, respectively) between aa 430 and aa 433 of L1, respectively. The chimeric L1 genes were expressed from recombinant baculoviruses in insect Sf9 cells, and three resultant purified preparations were designated as Ch18/38, Ch56/75, and Ch96/115(101L, 112S), respectively.

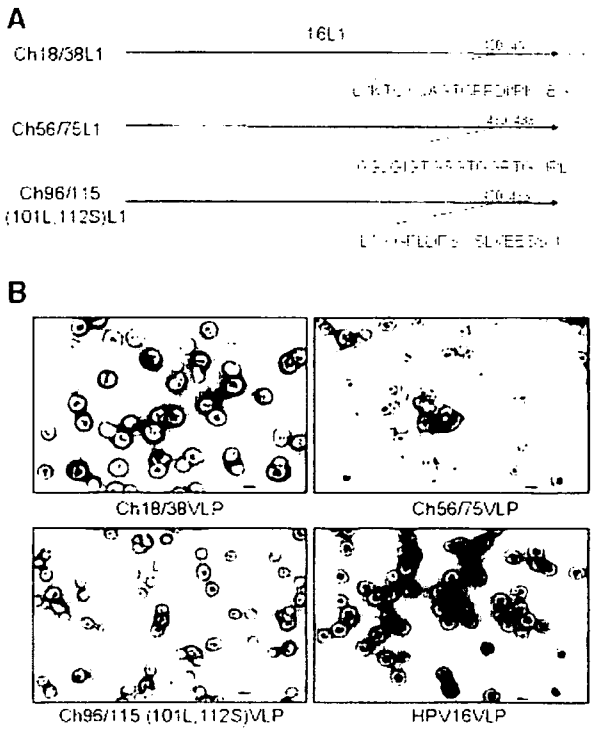

Fig. 1. **A**: Schematic representation of the chimeric L1 constructed in this study. The indicated amino acid sequences were inserted into HPV16 L1 between amino acids (aa) 430 and 433. The aa sequences inserted to Ch18/38 and Ch56/75 correspond to HPV16 L2 aa positions of 18–38 and 56–75, respectively. The aa sequences inserted into Ch96/115(101L, 112S) correspond to HPV16 L2 aa 96 to 115 with two replacement; S at aa 101 and T at aa 112 were replaced with L and S, respectively to convert the original aa into those of majority of the oncogenic HPVs. **B**: Electron micrographs of chimeric L1-capsids. The purified VLPs were allowed to settle on carbon-coated copper grids and negatively stained with 4% uranylacetate. The grids were examined in a HITACHI model H-7600 transmission electron microscope and photographed at an instrumental magnification of 200,000×. Bar = 50 nm.

The morphology of the resultant chimeric VLPs was examined under a transmission electron microscope (Fig. 1B). Ch18/38 was composed of spherical particles slightly larger than HPV16VLPs (a diameter of 55 nm). Ch56/75 was composed of particles with diameters of 40–55 nm and heterogeneous rod-shaped tubular structures. Ch96/115(101L, 112S) was composed of particles smaller than HPV virions. The results indicate that the insertions did not disturb the assembly of VLPs.

Display of the Inserted Peptides on the Chimeric VLPs

The anti-peptide antibodies, which were previously produced by immunizing rabbits with the synthetic peptides having the amino acid sequences identical to those of the peptides inserted into the chimeric L1s [Kondo et al., 2007], bound to the chimeric VLPs (Table I). The purified HPV16VLP and the chimeric VLPs were used as the antigens of ELISA. Anti-P18/38, anti-P56/75, and anti-P96/115(101L, 112S) exclusively

TABLE I. Binding of the Antibodies Against the Inserted-Peptides to the Chimeric VLPs (Absorbancy in ELISA With Serum Diluted at 1:500)

	Antigen			
Antiserum	HPV16VLP	Ch18/38VLP	Ch56/75VLP	Ch96/115(101L, 112S)VLP
Anti-P18/38	0.042	0.872	0.037	0.042
Anti-P56/75	0.041	0.039	0.803	0.041
Anti-P96/115(101L, 112S)	0.040	0.043	0.045	0.821

bound to Ch18/38, Ch56/75, and Ch96/115(101L, 112S), respectively (Table I), indicating that the peptides inserted into the chimeric L1s are displayed on the surface of the chimeric VLPs.

Induction of Antibody Against the Inserted Peptides by Immunization of Rabbits With the Chimeric VLPs

We examined antisera obtained by immunizing rabbits with each of Ch18/38, Ch56/75, and Ch96/115(101L, 112S) VLPs for binding to the synthetic peptides with aa sequences of the inserted peptides by using the peptides as the antigens of ELISA (Table II). Anti-Ch18/38#1 and #2 bound to HPV16VLP and P18/38. Anti-Ch56/75#1, #2, #3, and #4 bound to the HPV16 VLP and P56/75. The titer of anti-Ch56/75#2 appeared to be lower than those of the other anti-Ch56/75 sera. Anti-Ch96/115(101L, 112S)#1 and #2 bound to the HPV16VLP and P96/115(101L, 112S). The data indicate that the chimeric VLPs induced antibodies capable of binding to the peptides inserted into the chimeric L1s.

Neutralization of HPV16, 18, 31, 52, and 58 With Rabbit Anti-Chimeric-VLP Antisera

Neutralizing activity of the sera was evaluated from the reduction of infectivity of the pseudovirions that had been incubated with the diluted sera (Table III). All the pre-immune sera did not neutralize any of HPV16, 18, 31, 52, and 58 pseudovirions (data not presented).

Anti-chimeric-VLP sera, except for anti-Ch56/75#2, neutralized HPV16 pseudovirions highly efficiently. The neutralizing titers were comparable to the titer of anti-HPV16VLP rabbit serum, indicating that the major type-specific neutralization epitope(s) on the HPV16VLP is retained in the chimeric VLPs.

Anti-Ch18/38#1 and #2 cross-neutralized HPV18 and 31. Anti-Ch18/38#1 cross-neutralized HPV31 (titer 3,200) much more efficiently than anti-Ch18/38#2 (titer 50), suggesting that the two sera contained different sets of antibodies.

Anti-Ch56/75#1, #3, and #4 cross-neutralized HPV18, 31, 52, and 58 with various efficiency. Anti-Ch56/75#1 and #4 contained the antibody cross-neutralizing HPV52 and 58 efficiently and anti-Ch56/75#3 contained the antibody cross-neutralizing HPV18 efficiently. Anti-Ch56/75#2, whose level of binding to P56/75 was low (Table II), cross-neutralized HPV31, 52, and 58 but not HPV18, suggesting that anti-Ch56/75#2 contained a low level of the antibody included in anti-Ch56/75#1 and #4.

Anti-Ch96/115(101L, 112S)#1 cross-neutralized HPV18, 31, and 58. Anti-Ch96/115(101L, 112S)#2, whose neutralization titer against HPV16 was a half of that of anti-Ch96/115(101L, 112S)#1, cross-neutralized HPV18 and 31 but not HPV58.

The data indicate that the chimeric VLPs induced neutralizing antibody against HPV16, as HPV16VLP did, and were able to induce cross-neutralizing antibodies. The neutralization titers varied among immunized rabbits.

DISCUSSION

In this study we produced chimeric HPV16 L1 by inserting the peptides containing the cross-neutralizing L2-epitopes between aa 430 and 433. The chimeric L1s

TABLE II. Binding of the Anti-Chimeric-VLP Sera to the Inserted-Peptides (Absorbancy in ELISA With Serum Diluted at 1:500 for the Peptide Antigens and at 1:2,000 for HPV16VLP)

		Antigen	Peptide		
Antiserum		HPV16VLP	P18/38	P56/75	P96/115(101L, 112S)
Anti-Ch18/38	#1	0.711	0.543	0.041	0.042
	#2	0.633	0.402	0.039	0.039
Anti-Ch56/75	#1	0.844	0.040	0.965	0.039
	#2	0.354	0.037	0.135	0.042
	#3	0.923	0.043	1.034	0.045
	#4	0.854	0.042	0.972	0.041
Anti-Ch96/115(101L, 112S)	#1	0.765	0.041	0.045	0.421
	#2	0.590	0.043	0.042	0.380

TABLE III. Neutralization of HPV16, 18, 31, 52, and 58 Pseudovirions With the Anti-Chimeric-VLP Sera

		Neutralizing titer				
Antiserum		HPV16	HPV18	HPV31	HPV52	HPV58
Anti-Ch18/38	#1	204,800	400	3,200	<50	<50
	#2	102,400	200	50	<50	<50
Anti-Ch56/75	#1	51,200	200	3,200	6,400	1,600
	#2	1,600	<50	50	400	50
	#3	51,200	800	50	50	400
	#4	409,600	100	800	6,400	400
Anti-Ch96/115(101L, 112S)	#1	204,800	100	800	<50	50
	#2	102,400	50	50	<50	<50
Anti-HPV16VLP		204,800	<50	800	<50	<50

were able to assemble themselves into the chimeric VLPs (Fig. 1). The inserted peptides were displayed on the surface of the VLPs (Table I). Rabbit antisera obtained by immunization with the VLPs neutralized HPV16 efficiently, indicating that the chimeric VLPs retained immunogenicity of HPV16VLP (Table III). The antisera included antibodies recognizing the L2-epitopes (Table II) and the spectrum of the cross-neutralization (Table III) was consistent with that of the antiserum obtained by immunizing rabbits with the L2-peptides previously [Kondo et al., 2007]. Anti-Ch56/75 evidently cross-neutralized HPV18, 52, and 58 because the anti-HPV16VLP serum did not cross-neutralize these HPVs (Table III). Contribution of anti-L2 antibody to the neutralization of HPV31 was not clear because the anti-HPV16VLP serum cross-neutralized HPV31 (Table III).

The use of chimeric VLPs having the L2-epitopes as a vaccine antigen seems a practical strategy for induction of the cross-neutralizing antibody because dendritic cells incorporate VLPs efficiently and induce strong helper T-cell response [Yang et al., 2004; Fausch et al., 2005]. Recently, Slupetzky et al. [2007] reported that chimeric BPV1 L1 having the insertion of HPV16 L2-peptide of aa 69–81 or aa 108–120 into L1 between aa 133 and 134 formed capsomere or VLP, respectively. Immunization of rabbits with these constructs induced the L2-specific serum antibody with titers 10-fold higher than those induced by the cognate synthetic L2-peptides conjugated with KLH.

Although the sizes of the VLPs were not identical with that of HPV16VLP, the chimeric VLPs seemed much more stable than the other HPV16-based chimeric VLPs previously produced [Varsani et al., 2003; Slupetzky et al., 2007]. Varsani et al. [2003] inserted HPV16 L2-peptide of aa 108-120 into L1 between aa 81 and 93, aa 174 and 186, aa 131 and 143, aa 414 and 426, and aa 431 and 443. These chimeric L1 formed mainly aggregates.

Each rabbit antiserum obtained by immunization with Ch18/38 and Ch56/75 showed large diversity of relative cross-neutralization efficiency against HPV18, 31, 52, and 58. Probably the L2-peptides displayed on the chimeric VLPs contain more than one epitope, and the rabbits recognized these epitopes differently. The presence of the multiple epitopes might explain at least partly the large variation (from 50 to 6,400) of the neutralization titers of anti-Ch56/75 against HPV52. More studies on the epitopes are needed to elucidate the immunoresponse of individual rabbits to the chimeric VLPs.

The level of the anti-L2 neutralizing antibodies required for protecting humans from HPV infection is not clear at present. Accumulating data suggest that anti-L2 neutralizing antibody efficiently protect model animals from experimental challenge. The titer of the anti-L2 antibodies that protected the immunized animals ranged from an undetectable level to 1:256 by in vitro neutralization test with pseudovirions [Gaukroger et al., 1996; Embers et al., 2002; Gambhira et al., 2007]. These data encourage us to develop a new HPV vaccine capable of inducing anti-L2 cross-neutralizing antibody. Detailed analysis of the L2-epitopes will help develop the chimeric VLP vaccine inducing the antibody against the selected epitope that is the most effective for the cross-neutralization.

ACKNOWLEDGMENTS

We thank Dr. Kunito Yoshiike for critical reading of the manuscript.

REFERENCES

Buck CB, Pastrana DV, Lowy DR, Schiller JT. 2004. Efficient intracellular assembly of papillomaviral vectors. J Virol 78:751–757.

Clifford G, Franceschi S, Diaz M, Munoz N, Villa LL. 2006. Chapter 3: HPV type-distribution in women with and without cervical neoplastic diseases. Vaccine 24:S26–S34.

Embers ME, Budgeon LR, Pickel M, Christensen ND. 2002. Protective immunity to rabbit oral and cutaneous papillomaviruses immunization with short peptides of L2, the minor capsid protein. J Virol 76:9798–9805.

Fausch SC, Da Silva DM, Kast WM. 2005. Heterologous papillomavirus virus-like particles and human papillomavirus virus-like particle immune complexes activate human Langerhans cells. Vaccine 23:1720–1729.

Ferlay J, Bray F, Pisani P, Parkin DM. 2004. GLOBOCAN 2002: Cancer incidence. Mortality and prevalence worldwide. Lyon: IARC Press.

Gambhira R, Jagu S, Karanam B, Gravitt PE, Culp TD, Christensen ND, Roden RBS. 2007. Protection of rabbits against challenge with

rabbit papillomaviruses by immunization with the N-terminal of minor antigen L2. J Virol 81:11585–11592.

Gaukroger JM, Chandrachud LM, O'Neil BW, Grindlay GJ, Knowles G, Campo MS. 1996. Vaccination of cattle with bovine papillomavirus type 4 L2 elicits the production of virus-neutralizing antibodies. J Gen Virol 77:1577–1583.

Giroglou T, Sapp M, Lane C, Fligge C, Christensen ND, Streeck RE, Rose RC. 2001. Immunological analyses of human papilloma virus capsids. Vaccine 19:1783–1793.

Harper DM, Franco DM, Wheeler CM, Moscocki AB, Romanoswski B, Roteli-Martins CM, Jenkins D, Schuind A, Costa Clemens SA, Dubin G, HPV Vaccine Study Group. 2006. Sustained efficacy up to 4.5 years of a bivalent L1 virus-like particle vaccine against human papillomavirus types 16 and 18: Follow-up from a randomised control trial. Lancet 367:1247–1255.

Kirnbauer R, Booy F, Cheng N, Lowy DR, Schiller JT. 1992. Papillomavirus L1 major capsid protein self-assembles into virus-like particles that are highly immunogenic. Proc Natl Acad Sci USA 89:12180–12184.

Kirnbauer R, Taub J, Greenstone H, Roden R, Duerst M, Gissmann L, Lowy DR, Schiller JT. 1993. Efficient self-assembly of human papillomavirus type 16 and L1-L2 into virus-like particles. J Virol 67:6929–6936.

Kondo K, Ishii Y, Ochi H, Matsumoto T, Yoshikawa H, Kanda T. 2007. Neutralization of HPV16, 18, 31, and 58 pseudovirions with antisera induced by immunizing rabbits with synthetic peptides representing segments of the HPV16 minor capsid protein L2 surface region. Virology 358:266–272.

Koutsky LA, Ault KA, Wheeler CM, Brown DR, Barr E, Alvarez FB, Chiacchierini LM, Jansen KU. 2004. A controlled trial of a human papillomavirus type16 vaccine. N Engl J Med 347:1645–1651.

Munoz N, Bosch FX, Castellsague X, Diaz M, Sanjose S, Hammouda D, Shah KV, Meijer CJLM. 2004. Against which human papillomavirus types shall we vaccinate and screen? Int J Cancer 111:278–285.

Pastrana DV, Buck CB, Pang YY, Thompson CD, Castle PE, FitzGerald DC, Kruger Kjaer S, Lowy DR, Schiller JT. 2004. Reactivity of human sera in a sensitive, high-throughput pseudovirus-based papillomavirus neutralization assay for HPV16 and H PV18. Virology 321:205–216.

Slupetzky K, Gambhira R, Culp TD, Shafti-Keramat S, Schellenbacher C, Christensen ND, Roden RBS, Kirnbauer R. 2007. A papillomavirus-like particle (VLP) vaccine displaying HPV16L2 epitopes induces cross-neutralizing antibodies to H PV11. Vaccine 25:2001–2010.

Trus BL, Roden RBS, Greenstone HL, Vrhel M, Schiller JT, Booy FP. 1997. Novel structural features of bovine papillomavirus capsid revealed by three-dimensional reconstruction to 9 Å resolution. Nat Struct Boil 4:413–420.

Varsani A, Williamson AL, de Villiers D, Becker I, Christensen ND, Rybicki EP. 2003. Chimeric human papillomavirus type16(HPV-16) L1 particles presenting the common neutralizing epitope for the L2 minor capsid protein of HPV-6 and HPV-16. J Virol 77:8386–8393.

Villa LL, Costa RL, Petta CA, Andrade RP, Ault KA, Giuliano AR, Wheeler CM, Koutsky LA, Malm C, Lehtinen M, Skjeldestad FF, Olsson SE, Steinwall M, Brown DR, Kurman RJ, Ronnett BM, Stoler MH, Ferenczy A, Harper DM, Tamms GM, Yu J, Lupinacci L, Railkar R, Taddeo FJ, Jansen KU, Esser MT, Sings HL, Saah AJ, Barr E. 2005. Prophylactic quadrivalent human papillomavirus (types 6, 11, 16, and 18) L1 virus-like particle vaccine in young women: A randomised double-blind placebo-controlled multicentre phase II efficacy trial. Lancet Oncol 6:271–278.

Volpers C, Schirmacher P, Streeck R, Sapp M. 1994. Assembly of the major and the minor capsid protein of human papillomavirus type 33 into virus-like particles and tubular structures in insect cells. Virology 200:504–512.

Yang R, Murillo FM, Cui H, Blosser R, Uematsu S, Takeda K, Akira S, Viscidi RP, Roden RB. 2004. Papillomavirus-like particles stimulate murine bone marrow-derived dendritic cells to produce alpha interferon and Th1 immune responses via MyD88. J Virol 78: 11152–11160.

THE JOURNAL OF BIOLOGICAL CHEMISTRY VOL. 282, NO. 10, pp. 7368–7375, March 9, 2007

CD1d Degradation in *Chlamydia trachomatis*-infected Epithelial Cells Is the Result of Both Cellular and Chlamydial Proteasomal Activity*

Received for publication, November 20, 2006, and in revised form, January 10, 2007 Published, JBC Papers in Press, January 10, 2007, DOI 10.1074/jbc.M610754200

Kei Kawana[‡§], Alison J. Quayle[¶], Mercedes Ficarra[¶], Joyce A. Ibana[¶], Li Shen[‖], Yukiko Kawana[‡], Huixia Yang[§¶], Luis Marrero[**], Sujata Yavagal[§], Sheila J. Greene[¶], You-Xun Zhang[‖], Richard B. Pyles[‡‡], Richard S. Blumberg[§§], and Danny J. Schust[‡1]

From the [‡]Division of Reproductive Biology, Department of Obstetrics and Gynecology, Boston Medical Center, Boston University School of Medicine, Boston, Massachusetts 02118, the [§]Department of Obstetrics, Gynecology and Reproductive Biology, Brigham and Women's Hospital, Harvard Medical School, Boston, Massachusetts 02115, the [¶]Department of Microbiology, Immunology, and Parasitology, Louisiana State University Health Sciences Center, New Orleans, Louisiana 70112, the [‖]Division of Infectious Diseases, Department of Medicine, Boston University School of Medicine, Boston, Massachusetts 02118, the [**]Gene Therapy Program, Louisiana State University Health Sciences Center, New Orleans, Louisiana 70112, the [‡‡]Department of Pediatrics and Experimental Pathology, Sealy Center for Vaccine Development, University of Texas Medical Branch, Galveston, Texas 77555, and the [§§]Division of Gastroenterology, Department of Medicine, Brigham and Women's Hospital, Harvard Medical School, Boston, Massachusetts 02115

Chlamydia trachomatis* is an obligate intracellular pathogen that can persist in the urogenital tract. Mechanisms by which *C. trachomatis* evades clearance by host innate immune responses are poorly described. CD1d is MHC-like, is expressed by epithelial cells, and can signal innate immune responses by NK and NKT cells. Here we demonstrate that *C. trachomatis* infection down-regulates surface-expressed CD1d in human penile urethral epithelial cells through proteasomal degradation. A chlamydial proteasome-like activity factor (CPAF) interacts with the CD1d heavy chain, and CPAF-associated CD1d heavy chain is then ubiquitinated and directed along two distinct proteolytic pathways. The degradation of immature glycosylated CD1d was blocked by the proteasome inhibitor lactacystin but not by MG132, indicating that degradation was not via the conventional proteasome. In contrast, the degradation of non-glycosylated CD1d was blocked by lactacystin and MG132, consistent with conventional cellular cytosolic degradation of *N*-linked glycoproteins. Immunofluorescent microscopy confirmed the interruption of CD1d trafficking to the cell surface, and the dislocation of CD1d heavy chains into both the cellular cytosol and the chlamydial inclusion along with cytosolic CPAF. *C. trachomatis* targeted CD1d toward two distinct proteolytic pathways. Decreased CD1d surface expression may help *C. trachomatis* evade detection by innate immune cells and may promote *C. trachomatis* persistence.

Chlamydia trachomatis serovars D–K are common obligate intracellular pathogens that infect the columnar epithelia of the human urogenital mucosa (1, 2). Infection most frequently occurs in the penile urethra or endocervix and causes acute inflammatory responses at these sites (1–3). Despite immune recognition of infection, *C. trachomatis* can persist within the host, and persistence is associated with more severe disease (2, 3). *C. trachomatis*-associated alterations in host immunity are thought to promote persistence, and these immunoevasive mechanisms may affect innate immune responses, adaptive immune responses, or both.

Mechanisms for evasion of adaptive responses by *C. trachomatis* have been described, including the down-regulation of MHC[2] class I heavy chain (HC) and β2-microglobulin (β2m) expression (4–7). Down-regulation appears to be the result of a novel chlamydial proteasome-like activity factor (CPAF) (4, 6). CPAF, composed of N-terminal (29 kDa) and C-terminal (35 kDa) fragments, is secreted from the chlamydial inclusion into the host cytosol and degrades the transcriptional factor RFX5 that would otherwise up-regulate promoters of MHC class I HC and β2m genes (4, 6). *C. trachomatis* also targets upstream stimulation factor-1 for CPAF-mediated degradation, resulting in the inhibition of interferon γ-inducible expression of MHC class II products (5). Cellular fractionation places CPAF into subfractions that differ from those containing the classic cytosolic proteasome subunits. Further, CPAF-associated proteasomal activity is inhibited by one cytosolic proteasome inhibitor, lactacystin, but not by other proteasome inhibitors (4, 6). These data indicate that CPAF has proteasomal activities distinct from those of the classic cytosolic proteasome.

* This work was supported by National Institutes of Health Grants U19AI061972 and AI046518 (to D. J. S., A. J. Q., and R. B. P.) and KD44319 (to R. S. B.). The costs of publication of this article were defrayed in part by the payment of page charges. This article must therefore be hereby marked "*advertisement*" in accordance with 18 U.S.C. Section 1734 solely to indicate this fact.

[1] To whom correspondence should be addressed: Division of Reproductive Endocrinology and Fertility, Dept. of Obstetrics, Gynecology and Women's Health, University of Missouri-Columbia School of Medicine, Columbia Regional Hospital, 402 Keene St., Third floor, Columbia, MO 65201. Tel.: 573-499-6044; Fax: 573-499-6063; E-mail: schustd@health.missouri.edu.

[2] The abbreviations used are: MHC, major histocompatibility complex; CPAF, chlamydial protease/proteasome-like activity factor; HC, heavy chain; β2m, β2-microglobulin; PURL, penile urethral epithelial cells; p.i., post infection; mAb, monoclonal antibody; IP, immunoprecipitation; IB, immunoblotting; NK, natural killer cells; NKT, natural killer T cells; ER, endoplasmic reticulum; LPS, lipopolysaccharide.

CD1d is an MHC-like glycoprotein that presents lipid antigen to natural killer T (NKT) cells (8–10). In humans, a specific subset of NKT cells expresses an invariant Vα24-JαQ/Vβ11 T cell receptor and can recognize CD1d on the surface of antigen presenting cells through this receptor (9). Like MHC class I HC, CD1d HC is synthesized, glycosylated by *N*-glycosyltransferase, modified, and assembled with β2m within the endoplasmic reticulum (ER) (10–12). Unlike MHC class I HC, CD1d HC is not affected by quality control mechanisms that efficiently destroy misfolded *N*-linked membrane glycoproteins and those that have not properly assembled with β2m (10, 11, 13). In fact, diverse CD1d HC isoforms, including mature glycosylated (~48 kDa), immature glycosylated (~45 kDa), and non-glycosylated (~37 kDa) forms, are expressed on the cell surface in a cell-type specific fashion (10–12).

CD1d plays a role in both innate and adaptive immunity to various bacteria, viruses, fungi, and parasites (14, 15). Activation of CD1d-restricted invariant NKT cells enhances host resistance to these microbes. CD1d-restricted NKT cells can act directly on infected cells, killing the CD1d-expressing cell. They also promote interferon γ production by conventional NK cells and modulate adaptive immune cells by altering Th1/Th2 polarization. Recognition of CD1d by invariant NKT cells causes rapid release of interleukin-4 and interferon γ from the NKT cell (9). The activation of CD1d-restricted invariant NKT cells in response to microbial invasion is antigen-dependent, but these antigens can be derived from the invading microbe or possibly host antigens (16–18).

Viewing the importance of CD1d in innate immune responses to microbes, we hypothesized that *C. trachomatis* may alter CD1d-mediated immune pathways and thereby avoid innate immune destruction of the infected cell by the host. Here we demonstrate that surface-expressed CD1d in human urethral epithelial cells is down-regulated by *C. trachomatis* infection, and this involves both CPAF-mediated and classic cytosolic proteasomal pathways.

MATERIALS AND METHODS

Epithelial Cell Line—The PURL epithelial cell line was established from penile urethra collected at autopsy under IRB approval. Small pieces of tissue were cultured in supplemented keratinocyte growth media (Invitrogen) and 0.4 mM calcium until epithelial outgrowth occurred. Primary cells were transduced with a retroviral vector (LXSN-16E6E7) (22), selected by resistance to the neomycin analogue G418 and passaged over 20 times prior to experiments. The cytokeratin profile (positive for CK13, -17, and -18), and the expression of the secretory component of the polymeric immunoglobulin receptor (SC) confirmed derivation from penile urethral epithelium.

C. trachomatis Infection—Near confluent PURL cells were overlaid with *C. trachomatis* serovar F (strain F/IC-Cal-13) elementary bodies suspended in a sucrose-phosphate-glutamate solution at a predetermined dilution that resulted in 80–85% of cells becoming infected. Plates were centrifuged for 1 h, supernatants were aspirated after centrifugation, and cells cultured for up to 45 h at 37 °C in keratinocyte growth media.

Antibodies—For anti-CD1d antibodies, a D5 mAb (mIgG2b (11)) recognizing all isoforms of CD1d HC was used for biochemical experiments. An NOR3.2 mAb (mIgG1, Abcam Inc., Cambridge, MA) recognizing all isoforms was used for flow cytometry and immunofluorescence. A 51.1.3 mAb (mIgG2b (10)) recognizing only mature glycosylated-CD1d was used for immunofluorescence. For anti-CPAF antibodies, an n54b mAb (mIgG1 (6)) recognizing N terminus and a c100a mAb (mIgG1 (7)) recognizing C terminus fragments of CPAF (kind gifts from Dr. G. Zhong, University of Texas, San Antonio, TX) were used for immunoprecipitation and immunoblotting, respectively. The n54b mAb was also used for immunofluorescence.

Flow Cytometry—PURL cells infected with *C. trachomatis* were harvested 24 h after infection. Uninfected and infected PURL cells were harvested using accutase (Chemicon, Temecula, CA). Harvested cells were then incubated with an anti-transferrin receptor mAb conjugated to phycoerythrin (Caltag Laboratories) or with an anti-CD1d NOR3.2 mAb for 30 min at 4 °C. CD1d staining was followed by a goat anti-mouse Ig secondary antibody conjugated to phycoerythrin for 30 min at 4 °C (BD Biosciences, San Jose, CA). Cells were suspended in 1% paraformaldehyde and analyzed using a FACSCalibur flow cytometry system (BD Biosciences).

Proteasome Inhibitor Treatment—Infected and control PURL cells were cultured for up to 45 h in the presence or absence of two different cytosolic proteasome inhibitors: lactacystin (2 or 10 μM) or MG132 (2 or 10 μM, Sigma-Aldrich) in Me_2SO. Control wells included vehicle alone.

Immunoprecipitation and Western Immunoblotting—Harvested PURL cells were lysed in modified radioimmune precipitation assay buffer (1% Nonidet P-40, 1% deoxycholate, 0.1% SDS, 10 mM Tris, 150 mM NaCl, 2 mM EDTA) with protease inhibitors (Amersham Biosciences). Equivalent aliquots of cell lysates were incubated overnight at 4 °C with 5 μg/ml of anti-CD1d D5 mAb or anti-CPAF n54b and 5 μl of Protein-A-Sepharose (Amersham Biosciences). Precipitated proteins were separated by SDS-PAGE using 8 or 10% acrylamide gels and transferred to polyvinylidene difluoride membranes. Purified CPAF c-fragment proteins (a kind gift from Dr. G. Zhong, University of Texas, San Antonio, TX) were included as positive controls. Anti-CD1d D5 mAb, anti-CPAF c100a mAb, or a rabbit anti-β-actin polyclonal antibody (Abcam Inc.) were used as primary reagents for immunoblotting and peroxidase-conjugated goat anti-mouse or anti-rabbit IgG antibodies (Pierce) as secondary reagents. A peroxidase-conjugated mouse anti-ubiquitin antibody (P4D1, Santa Cruz Biotechnology, Santa Cruz, CA) was used to detect ubiquitin. Products in Western immunoblotting experiments were visualized using standard chemiluminescence (Amersham Biosciences). Molecular weights were confirmed by comparison to standard size markers and molecular weight analysis (FluorChem™SP. Alpha Innotech, San Leandro, CA).

Endoglycosidase-H Treatment—D5-precipitated CD1d HCs were denatured and incubated overnight at 37 °C with endoglycosidase-H (New England Biolabs, Beverly, MA) in reaction

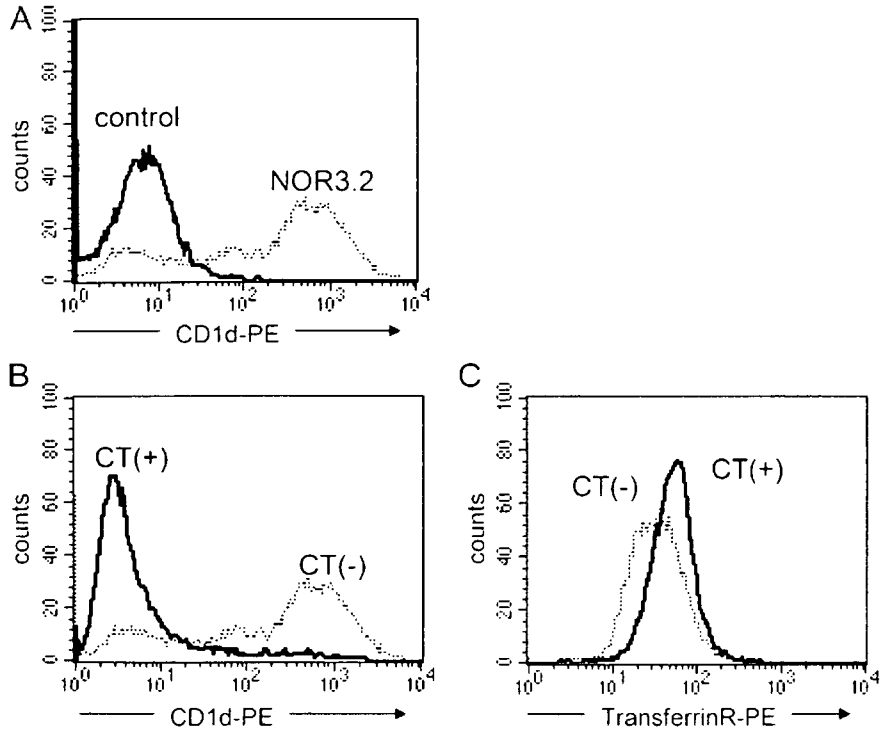

FIGURE 1. ***C. trachomatis* infection down-regulates CD1d surface expression in PURL cells.** *A*, CD1d expression on uninfected PURL cells. Background level staining of the cells with secondary antibody is also shown (*control*). *B*, CD1d expression on PURL cells harvested 24 h post infection with *C. trachomatis* serovar F (*CT(+)*) and uninfected cells (*CT(−)*). The PURL cells were stained with the NOR 3.2 anti-CD1d antibody and a phycoerythrin conjugated goat anti-mouse Ig secondary antibody. *C*, transferrin receptor expression on *C. trachomatis*-infected and uninfected PURL cells. *CT*, *C. trachomatis*.

buffer (11). Protein products were analyzed by Western immunoblotting.

Immunoprecipitation by a His-tagged, Synthetic CD1d Cytoplasmic Tail—Three polypeptides with sequences corresponding to the wild-type CD1d cytoplasmic tail (HHHHHH-RFKRQTSY-QGVL), to a mutated cytoplasmic tail lacking tyrosine and lysine residues (HHHHHH-RFKRQTS*F*QGV*A*), or to a truncated cytoplasmic tail lacking six amino acids (HHHHHH-RFKRQT) (20) were synthesized, His tag conjugated, and purified by high-performance liquid chromatography (New England Peptide, Inc., Gardner, MA). Total cell lysates were incubated with or without the synthesized peptides (0, 20, or 100 μg) in 200 μl of radioimmune precipitation assay buffer for 2 h at 4 °C. Bound proteins were recovered using anti-His tag antibody-conjugated agarose beads (Abcam Inc.), separated by PAGE and immunoblotted with the anti-CPAF c100a mAb.

Fluorescence Deconvolution Microscopy—PURL cells were seeded onto coverslips and infected as above. The ER was visualized using ER tracker Blue-White DPX (Molecular Probes, Eugene, OR) for 30 min at 37 °C. All coverslips were fixed in 4% paraformaldehyde, permeabilized with 0.1% Tween 20, and incubated for 2 h at 37 °C with anti-CD1d 51.1.3 mAb, anti-CD1d NOR3.2 mAb, or anti-CPAF n54b mAb singly, or in combination with anti-chlamydial LPS (clone-3, Accurate, Westbury, NY). Alexa Fluor 568-conjugated anti-mouse IgG1 (51.1.3, NOR3.2, and n54b) or Alexa Fluor 488-conjugated anti-mouse IgG3 (chlamydial LPS) were used as secondary reagents. In some experiments NOR3.2 was directly conjugated with Zenon Alexa Fluor 488 using a mouse IgG1 labeling kit (Molecular Probes) to allow costaining with CPAF. Thereafter, except in ER-Tracker-treated coverslips, cells were counterstained with a 4′,6-diamidino-2-phenylindole (Molecular Probes) nucleic acid stain. Images were obtained with a Leica DMRXA automated upright epifluorescence microscope (Leica Microsystems, Bannockburn, IL); a Sensicam QE charge-coupled device (Cooke Corp., Auburn Hills, MI); and filter sets optimized for Alexa 488 (exciter HQ480/20, dichroic Q495LP, and emitter HQ510/20m), Alexa 568 (exciter 545/30x, dichroic Q570DLP, emitter HQ620/60m), and 4′,6-diamidino-2-phenylindole (exciter 360/40×, dichroic 400DCLP, and emitter GG420LP). Z-axis plane capture, deconvolution, and analysis were performed with Slidebook™ deconvolution software (Intelligent Imaging Innovations, Denver, CO).

RESULTS

To determine how *C. trachomatis* infection affects CD1d expression, flow cytometry was used to analyze its cell-surface expression on PURL epithelial cells, a cell line we immortalized from penile urethra, the most common site of infection in the male. Cells were infected with *C. trachomatis* serovar F in this, and all subsequent experiments, because it is one of the most frequent genital isolates. We observed that CD1d was expressed by the majority of uninfected PURL cells; however, by 24 h post infection, CD1d expression was abrogated in >90% of cells in the *C. trachomatis*-infected cultures (Fig. 1*B*). The loss of CD1d expression was selective, because PURL cells retained, and in fact showed a slight increase in, their expression of transferrin receptor (Fig. 1*C*). PURL cells were then infected with *C. trachomatis* and harvested at various time points (up to 45 h after infection) to biochemically assess the effects of *C. trachomatis* infection on CD1d HC. All isoforms of CD1d HC were recovered using an anti-CD1d mAb (D5) that recognizes the α-region of the CD1d HC regardless of its association with β2m (10, 11). The anti-CD1d D5 mAb precipitated CD1d HC isoforms of ~48 kDa (*open arrowhead*), 45 kDa (*closed arrow*), and 37 kDa (*open arrow*) with distinct patterns depending on infection status and time after *C. trachomatis* infection. (Fig. 2*A*, *panel 1*). In non-infected PURL cells, the 48-kDa CD1d HC predominated, whereas the 45- and 37-kDa forms were present in negligible amounts (*panel 1*, *lane 1*).

CD1d isoforms were altered in the presence of *C. trachomatis* infection in a time-dependent, stepwise fashion (Fig. 2*A*, *panel 1*). The 48-kDa HC was largely converted to a 45-kDa HC

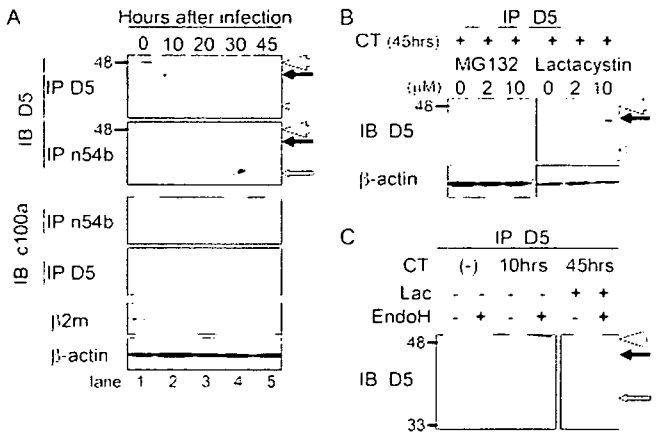

FIGURE 2. **CD1d HC degradation upon *C. trachomatis* infection.** *A*, PURL cells were infected with *C. trachomatis* and harvested at 0, 10, 20, 30, and 45 h p.i. Total cell lysates were subjected to IP using anti-CD1d (*D5*) or anti-CPAF n-fragment (*n54b*) mAbs. Precipitated proteins were separated by PAGE and immunoblotted with anti-CD1d (*D5*) or anti-CPAF c-fragment (*c100a*) mAbs. The mAb pairs (D5–D5, n54b–D5, n54b–c100a, or D5–c100a) when used sequentially for IP and IB, isolated total CD1d HC, CPAF-bound CD1d HC, total CPAF, or CD1d-bound CPAF, respectively. *Open arrowheads, closed arrows,* and *open arrows* indicate the 48-, 45-, and 37-kDa HC bands, respectively. Protein levels of β2m and β-actin (loading control) in total cell lysates were detected by Western immunoblotting. *B*, PURL cells were infected as in *A* and exposed to the proteasome inhibitors, MG132 (*left*) or lactacystin (*right*) at the indicated concentrations for 45 h. Total cell lysates were used for IP and IB with the anti-CD1d (D5) mAb as in *A*. *Arrow/arrowheads* indicate HC bands as in *A*. *C*, D5-precipitated proteins from *C. trachomatis*-infected and non-infected lactacystin (*Lac*)-treated cells were treated with endoglycosidase-H (*EndoH*). Endoglycosidase-H-treated and control proteins were used for IP and IB with the anti-CD1d (*D5*) mAb as in *A*. *Arrow/arrowheads* indicate HC bands as in *A*. *CT, C. trachomatis*.

form between 10 to 20 h post infection (p.i.), and this was accompanied by a decrease in β2m protein levels (Fig. 2*A*, *panels 1* and *5*). To confirm the glycosylation status of the 45-kDa HC, the isoform was digested by endoglycosidase-H (Fig. 2*C*). The 45-kDa CD1d HC was sensitive to endoglycosidase-H and represents an immature glycosylated CD1d that may include β2m-unassembled HCs.

The amount of detectable, 45-kDa, glycosylated CD1d HC protein decreased by 20 h p.i. By 30 h p.i., it was no longer detectable. In its place, a 37-kDa non-glycosylated CD1d HC form began to accumulate at 20 h p.i. This isoform predominated at 30 h but was nearly undetectable by the end of the infectious cycle.

We hypothesized that the degradation of CD1d HCs in the presence of *C. trachomatis* infection may involve the *C. trachomatis*-specific proteasomal activity, CPAF (6). To address this possibility, we used coimmunoprecipitation (IP) to search for physiologic interactions between CPAF and CD1d HCs (Fig. 2*A*, *panels 2–4*). Using combinations of the anti-CD1d D5 mAb and mAbs against the C-terminal (c100a) or N-terminal (n54b) fragments of CPAF we could demonstrate association between CPAF and CD1d and follow these associations through the infectious cycle. CPAF-bound proteins and CPAF itself were immunoprecipitated with the anti-CPAFn n54b mAb, separated by PAGE, and immunoblotted with anti-CD1d D5 (*panel 2*) or anti-CPAFc c100a (*panel 3*) mAbs. In turn, CD1d-associated proteins were recovered with the anti-CD1d D5 mAb, separated by PAGE and immunoblotted with anti-CPAFc c100a mAb (*panel 4*). Experiments using primary IP with anti-CD1d D5 and anti-CPAFn n54b mAbs demonstrated that CD1d HCs and CPAF interacted with each other physiologically (Fig. 2*A*, *panels 2* and *4*). Furthermore, CPAF preferentially associated with the 45-kDa immature glycosylated CD1d and 37-kDa non-glycosylated CD1d but not the 48-kDa mature glycosylated CD1d HC (Fig. 2*A*, *panel 2*). CPAF binding to CD1d HC was first detected at 20 h p.i. By 30 h p.i., the CPAF-associated immature glycosylated CD1d was undetectable. In parallel, the levels of the CPAF-associated non-glycosylated CD1d increased transiently at 30 h p.i. and decreased to nearly undetectable levels by 45 h p.i. Primary CPAF IPs (*panels 3* and *4*) confirmed the findings of primary CD1d IPs. CPAF was first detected at 10 h p.i., and the levels of total and CD1d-associated CPAF increased by 20 h p.i. and then decreased by 45 h p.i.

To assess the role of proteasomal activity in *C. trachomatis*-associated degradation of CD1d HC, *C. trachomatis*-infected cells were exposed to the cytosolic proteasome inhibitor, MG132 (*left panel*) and to lactacystin (*right panel*) (Fig. 2*B*). Total CD1d HC was detected by IP-IB with the anti-CD1d D5 mAb. In the absence of proteasomal inhibition, CD1d HCs could not be detected at 45 h p.i. In the presence of either MG132 or lactacystin, the 37-kDa non-glycosylated CD1d was detectable, and levels of this HC increased with increasing inhibitor dose. In turn, in the presence of lactacystin, but not MG132, the 45-kDa immature glycosylated CD1d could be detected, and levels of this HC increased with lactacystin dose. The rescued 45-kDa HC form was confirmed to be sensitive to endoglycosidase-H. The immature glycosylated CD1d HC was degraded without deglycosylation (Fig. 2*C*).

As illustrated in *panels 3* and *4* of Fig. 2*A*, CD1d-associated CPAF was no longer detectable by 45 h p.i., despite the continued presence of some CPAF protein. Indeed, CD1d-associated CPAF was rescued by both MG132 and lactacystin, indicating that at least the classic cytosolic proteasome is involved in the degradation of CPAF together with the CD1d HC (Fig. 3*A*).

Fractionation experiments have demonstrated that CPAF is localized to the cytosol and is active in this location (4, 6). However, neither properly assembled nor aberrant forms of CD1d are normally present in the cytosol (11, 12). Still, CD1d and CPAF interact physiologically. We hypothesized that CPAF associates with CD1d HCs via a site on the CD1d cytoplasmic tail. To address this hypothesis, we synthesized three peptides with amino acid sequences corresponding to the 12 amino acids that comprise the entire wild-type CD1d cytoplasmic tail (RFKRQTSYQGVL), to a mutated cytoplasmic tail lacking tyrosine and lysine residues (RFKRQTS*F*QGV*A*), and to a truncated cytoplasmic tail lacking six amino acids (RFKRQT) (20). All peptides were conjugated to a His tag. Total cell lysates from infected and control PURL cells were incubated with the synthetic His-tagged CD1d cytoplasmic tail, and peptide-associated proteins were recovered with an anti-His tag antibody. Western immunoblotting of the precipitated proteins demonstrated that CPAF interacted physically with the CD1d cytoplasmic tail, and these interactions occurred in a dose-dependent manner (Fig. 3*B*). In comparison to the CPAF band precipitated by the wild-type peptide (*wt*), CPAF was barely detectable after precipitation by the point-mutated peptide

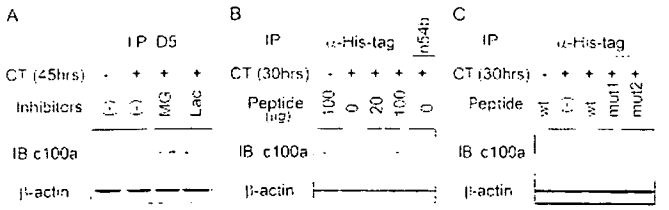

FIGURE 3. **CPAF rescue by proteasome inhibitors and CPAF interaction with CD1d.** *A*, PURL cells were infected as in Fig. 1*A* and exposed to 10 μM MG132, 10 μM lactacystin, or vehicle control for 45 h. CD1d-bound CPAF was immunoprecipitated with the anti-CD1d (D5) antibody. Immunoprecipitants were separated by PAGE and immunoblotted with the anti-CPAFc (c100a) mAb. β-Actin in total cell lysates (loading control) was detected separately using Western immunoblotting. *B*, an His tag-conjugated peptide with amino acid sequence corresponding to the entire cytoplasmic tail of the human CD1d HC was synthesized and purified by high-performance liquid chromatography. Various amounts of peptide (0, 20, or 100 μg per 200 μl of radioimmune precipitation assay buffer) were incubated with total cell lysates from non-infected and *C. trachomatis*-infected cells. Peptide-bound proteins were recovered with an anti-His tag antibody. Immunoprecipitants were separated by PAGE and immunoblotted with the anti-CPAFc c100a mAb. Precipitatants using the anti-CPAFn n54b mAb served as a positive control. *C*, 100 μg of three synthetic peptides (wild-type peptide (*wt*), a point-mutated peptide lacking tyrosine and lysine residues (*mut1*), or a truncated peptide lacking cytoplasmic six amino acids (*mut2*)), were used for peptide precipitations as in Fig. 3*B*. Immunoprecipitants were separated by PAGE and immunoblotted with the anti-CPAFc c100a mAb. *CT*, *C. trachomatis*.

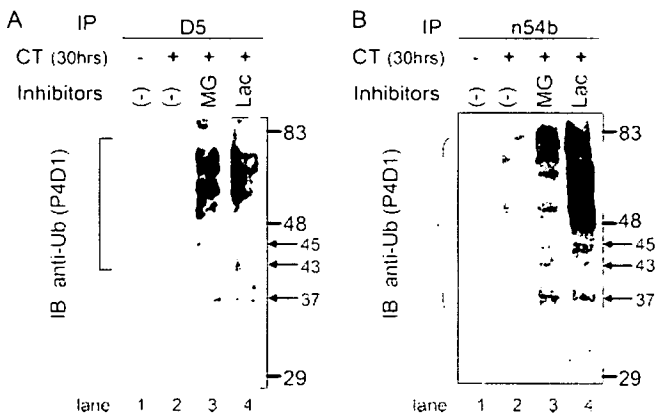

FIGURE 4. **CD1d HC and CPAF are ubiquitinated prior to degradation.** PURL cells were infected with *C. trachomatis* as in Fig. 1 and exposed to 10 μM of MG132 (*MG*), 10 μM lactacystin (*Lac*), or vehicle control for 30 h. Total cell lysates from non-infected and *C. trachomatis*-infected cells were immunoprecipitated with either anti-CD1d (*D5*) (*A*) or anti-CPAFn (*n54b*) mAbs (*B*) as described in Fig. 1*A*. Precipitated proteins were separated by PAGE and immunoblotted with a peroxidase-conjugated mouse anti-ubiquitin antibody (*P4D1*). *Closed arrows* indicate exact molecular weights. Standard molecular size markers are shown. Ubiquitinated CD1d/CD1d-associated proteins or CPAF/CPAF-associated proteins are shown using a *bracket* or *brace*, respectively. *CT*, *C. trachomatis*.

(*mut1*) and undetectable after precipitation with the truncated peptide (*mut2*) (Fig. 3*C*). These data suggest that CPAF interacts directly or indirectly to CD1d HC via sites on the CD1d cytoplasmic tail.

The classic cellular proteasome requires ubiquitination of host *N*-linked glycoproteins prior to their degradation (21). PURL cells were infected with *C. trachomatis* and exposed to proteasome inhibitors. Total cell lysates harvested at 30 h pi were subjected to IP with either anti-CD1d D5 (Fig. 4*A*) or anti-CPAFn n54b (Fig. 4*B*) mAbs. Immunoprecipitants were separated by PAGE and immunoblotted with a peroxidase-conjugated anti-ubiquitin antibody. Ubiquitinated CD1d HCs were not detected in non-infected cells (Fig. 4*A*, *lane 1*) and were

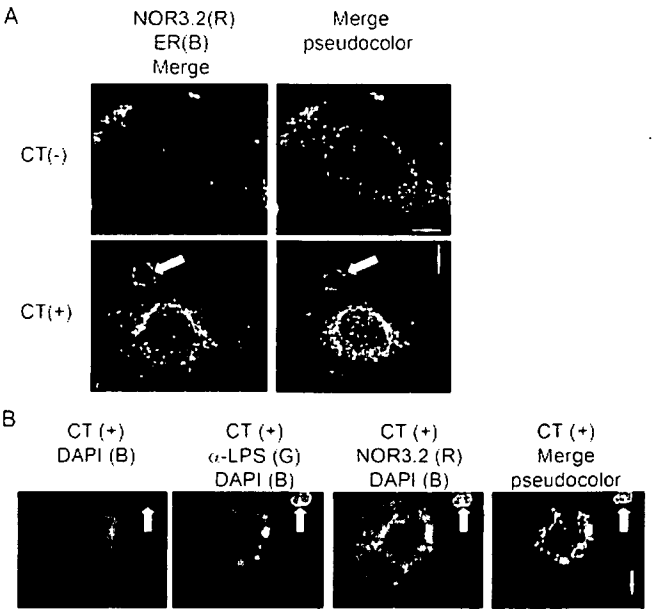

FIGURE 5. **Redistribution of CD1d HC in *C. trachomatis*-infected cells.** PURL cells were infected with *C. trachomatis* as described in Fig. 1*A*. At 24 h post infection. *A*, dual labeling of infected and control cells was performed with an anti-CD1d mAb (NOR3.2, *red*) and ER tracker (*blue*) and visualized by fluorescence deconvolution microscopy (*left panels*). Pseudocolor images represent the intensity of colocalization of the ER with respect to CD1d (*right panels*). The pseudocolor spectrum varies from *blue* (no colocalization) to *red* (full colocalization). *B*, the *C. trachomatis*-infected PURL cells were labeled with 4′,6-diamidino-2-phenylindole (*DAPI*, *blue*), anti-chlamydial LPS (*green*), and NOR3.2 (*red*) (*three left panels*). The pseudocolor image represents the intensity of colocalization of chlamydial LPS with respect to CD1d (*right panel*). *Arrows* indicate chlamydial inclusion. *CT*, *C. trachomatis*.

barely detectable in *C. trachomatis*-infected cells that were not exposed to proteasome inhibitors (Fig. 4*A*, *lane 2*). In contrast, in the presence of proteasome inhibitors, ubiquitinated proteins accumulated in *C. trachomatis*-infected cells. Use of protein size markers and size analysis confirmed that the molecular weights of the ubiquitinated CD1d and CPAF bands were as expected. Ubiquitinated CD1d HCs were observed as a ladder of signals with molecular masses greater than ~45 kDa (Fig. 4*A*, *lanes 3* and *4*). The 37- and 43-kDa bands may represent ubiquitinated proteins coprecipitated with CD1d, possibly including ubiquitinated CPAF N and C terminus fragments (Fig. 4*A*). Ubiquitinated CPAF-associated proteins, including CD1d HCs, were observed as a ladder of signals with molecular masses greater than ~45 kDa (Fig. 4*B*, *lanes 3* and *4*). The amounts of ubiquitinated CPAF or CPAF-associated proteins, including CD1d HCs, were greater after exposure to lactacystin than to MG132 (Fig. 4, *A* and *B*).

To visually document the effect of *C. trachomatis* infection on CD1d intracellular trafficking, immunofluorescence microscopy was first performed with an anti-CD1d mAb (NOR3.2) that reacts with total CD1d HCs and either an ER-specific marker (ER tracker) or an anti-chlamydial LPS mAb (Fig. 5). In non-infected PURL cells, NOR3.2-reactive CD1d was detected throughout the intracellular space, with increased accumulation near the cell surface (Fig. 5*A*, *upper images*). In contrast, the majority of CD1d molecules in *C. trachomatis*-infected PURL cells localized to the perinuclear area near the ER (Fig. 5*A*, *lower images*). In addition, CD1d was present in

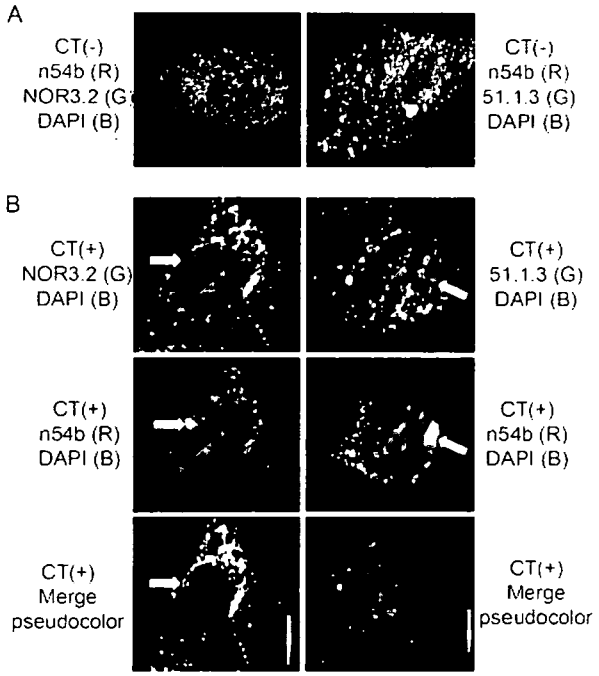

FIGURE 6. **CPAF distribution in *C. trachomatis*-infected cells.** PURL cells were infected with *C. trachomatis* as described in Fig. 1*A*. At 24 h post infection control cells (*A*) and infected cells (*B*) were costained with anti-CD1d (CD1d HC, NOR3.2-reactive (*left panels*) or properly folded mature glycosylated CD1d, 51.1.3-reactive (*right panels*)) mAbs (*green*), anti-CPAF (n54b) mAb (*red*), and 4′,6-diamidino-2-phenylindole (*blue*) and visualized by fluorescence deconvolution microscopy. Pseudocolor images in *B* represent the intensity of colocalization of CPAF with respect to CD1d. The pseudocolor spectrum varies from *blue* (no colocalization) to *red* (full colocalization). *Arrows* indicate chlamydial inclusion. *CT*, *C. trachomatis*.

infected cells in a distinct ring-shaped intracellular distribution that correlates morphologically with the chlamydial inclusion. CD1d and ER signals partially colocalized in the perinuclear area, suggesting that some forms of CD1d are present within the ER, but the majority of CD1d localized to the cytosol surrounding the ER (Fig. 5*A*, *right images*). Dual labeling for CD1d and chlamydial LPS verified the colocalization of CD1d and chlamydial elements within the chlamydial inclusion (Fig. 5*B*, *green* to *red pseudocolor*). These immunofluorescence microscopy studies thus support our flow cytometry and biochemical data that CD1d HC in *C. trachomatis*-infected cells fails to traffic efficiently to the cell surface. Rather, by 24 h p.i., the majority of CD1d HCs can be found in the cytosol near the ER, although some HCs localize within the ER and around chlamydial inclusion. CD1d HC appears to be targeted toward two degradation pathways: one ER-associated and one *Chlamydia*-mediated.

The anti-CD1d 51.1.3 mAb preferentially recognizes a conformational epitope associated with CD1d maturity (10, 11). This allowed us to discriminate the effects of *C. trachomatis* infection on properly folded mature glycosylated CD1d (51.1.3-reactive) from the effects on total CD1d HCs (NOR3.2-reactive) (Fig. 6). A pseudocolor rendering demonstrated moderate colocalization of CPAF and NOR3.2-reactive CD1d HC (Fig. 6*B*, *bottom left panel*) and confirmed our biochemical data showing the physiologic interaction of cytosolic CPAF with the CD1d HC. The distribution of the CPAF-CD1d complex was similar to that of total CD1d HC shown in Fig. 5. In the *right panel* of Fig. 6*A*, 51.1.3-reactive mature glycosylated CD1d is again noted throughout the intracellular space and on the cell surface in uninfected cells. By 24 h p.i., mature glycosylated CD1d localized almost exclusively to the perinuclear area (Fig. 6*B*, *right panels*). Signals for CPAF also localize to the perinuclear area and in the area of the chlamydial inclusion. Pseudocolor rendering (*bottom right panel*) indicated that there is no colocalization of CPAF with 51.1.3-reactive mature glycosylated CD1d. These patterns differed significantly from those for NOR3.2-reactive CD1d HC (*left panels*) and demonstrate that mature glycosylated CD1d is neither bound to CPAF nor associated with the chlamydial inclusion.

DISCUSSION

This study demonstrates that CD1d molecules are decreased on the surface of *C. trachomatis*-infected cells, although CD1d mRNA levels were not altered when compared with those in non-infected cells (data not shown). The three described isoforms of CD1d HC protein were here observed in distinctive patterns that depended upon the infection status and the time after *C. trachomatis* infection. The 45-kDa glycosylated CD1d HC, rather than the 48-kDa mature glycosylated CD1d HC, is the predominant isoform present between 10 and 20 h p.i. This was accompanied by a decrease in β2m protein levels. The reduction in recoverable β2m in *C. trachomatis*-infected cells has been reported to result from degradation of the transcription factor, RFX5, by CPAF (4). Zhong G *et al.* reports that CPAF is secreted into cytosol after 24 h of infection in HeLa cell (4, 6). The exact timing of the secretion of CPAF in our experiments may be characteristic of our infected cell type and the infecting *C. trachomatis* serovar and may therefore differ from the timing seen in similar experiments performed by others. Here, CPAF secretion started at 10 h p.i. and accumulated in the cytosol by 24 h p.i. as demonstrated visually in Fig. 6. Because the effect of CPAF on β2m through RFX5 is very rapid (within 30 min) (4), the appearance of CPAF at 10 h p.i. could result in our observed decrease in β2m between 10 to 20 h p.i. In β2m-deficient cells, surface-expressed CD1d HCs are glycosylated, but their carbohydrate side chains are incompletely modified. These CD1d HCs migrate at ~45 kDa (11), as do the β2m-unassembled immature glycosylated CD1d shown in our experiments. Notably, CD1d HC carbohydrate modification and trafficking to the cell surface is delayed in β2m-deficient cells (11). This effect is consistent with our immunohistochemical data. The delayed exit of immature glycosylated CD1d from the ER should facilitate CPAF-associated direction of CD1d to degradation. Finally cell-surface CD1d was clearly down-regulated in *C. trachomatis*-infected cells analyzed by flow cytometry.

The classic cellular proteasome requires removal of *N*-linked glycans from aberrant cytosolic glycoprotein targets prior to their degradation (13). However, in our experiments, lactacystin rescued a 45-kDa CD1d HC that remained sensitive to endoglycosidase-H. This immature glycosylated CD1d HC appears to be degraded without deglycosylation. Because MG132 was not able to rescue this immature glycosylated CD1d isoform, we propose that it is degraded by CPAF rather than by the classic cellular proteasome.

CD1d Degradation upon Chlamydia Infection

In contrast, the 37-kDa non-glycosylated isoform of CD1d was rescued by both proteasome inhibitors. Because the CPAF-mediated proteolytic pathway can't be inhibited by MG132 (4), the non-glycosylated 37-kDa CD1d HC must be degraded at least partially by the classic cytosolic proteasome. The degradation process for this isoform, including ubiquitination and deglycosylation, suggest it represents an intermediate in the classic proteolytic pathway for degrading aberrant *N*-linked glycoproteins (13, 21). The *C. trachomatis*-infected epithelial cells shown here represent the first model system to allow detection of all three isoforms of the CD1d HC. The experimental system suggests that all isoforms may be pathophysiologically relevant.

Immunostaining data support a model in which CPAF binds to immature glycosylated CD1d and non-glycosylated CD1d and dislocates them into the cytosol surrounding the ER and the chlamydial inclusion. Here, it is degraded in a CPAF-dependent manner that can be distinguished from pathways for classic cytosolic proteasomal degradation.

Interestingly, our ubiquitination experiments demonstrated that the amounts of ubiquitinated CPAF-associated proteins were greater after exposure to lactacystin than after exposure to MG132. However, there was no difference in the amount of rescued CPAF between exposure to MG132 and lactacystin (Fig. 3*A*). These data suggest that CPAF target proteins could be ubiquitinated prior to degradation by a CPAF-associated proteolytic pathway. Ubiquitinated CD1d HC could be degraded by both classic and CPAF-associated pathways, because those were rescued equally by MG132 and lactacystin. In initial descriptions of chlamydial proteasome-like activity, the authors noted the possibility that *C. trachomatis* could also co-opt cellular cytosolic proteolytic pathways to degrade host transcription factors (4, 6). Our data clearly demonstrate that *C. trachomatis* not only provides its own mechanism for CD1d degradation but also uses the classic proteolytic pathway for degrading aberrant *N*-linked glycoproteins to inhibit CD1d trafficking to the cell surface. CPAF is involved in both pathways.

We propose the following model for CD1d proteolysis in *C. trachomatis*-infected cells (Fig. 7). Cytosolic CPAF interacts with CD1d via cytoplasmic tail of the CD1d HC. This triggers dislocation of the CD1d HC into the cytosol where it is further processed along two distinct pathways. In one, glycosylated HC in the cytosol is ubiquitinated and deglycosylated. Ubiquitinated, deglycosylated CD1d and CPAF are directed toward degradation by the classic cytosolic proteasome. Immature glycosylated CD1d HC is degraded by CPAF-associated mechanisms that are distinct from those of the cytosolic proteasome.

Does *C. trachomatis* target CD1d HC for degradation as a means to evade immune recognition? In responses to some microbes, the rapid effects of CD1d-restricted NKT cells do not require recognition of microbial specific antigens (16–18). Instead, NKT cells can be activated in response to self-antigen presented by CD1d, and these actions are amplified by interleukin-12 derived from dendritic cells (16). Certainly, a reduced expression of CD1d at the cell surface could prevent *C. trachomatis*-infected cells from such an attack. It was recently demonstrated that Kaposi sarcoma-associated herpesvirus reduces cell-surface expression of CD1d via ubiquitination of the CD1d HC on its cytoplasmic tail (15). This, in turn, impairs CD1d-restricted T cell activation toward virally infected cells (15). Herpes simplex virus-1 down-regulates cell-surface CD1d expression by inhibition of CD1d recycling (22). Human immunodeficiency virus-1 Nef protein reduces cell-surface CD1d expression by binding to the cytoplasmic tail of CD1d HC, and this accompanies a decreased NKT cell activation (20). In *C. trachomatis*-infected PURL cells, CD1d degradation is accompanied by a suppression of CD1d-mediated cytokine secretion, including the production of interleukin-12.[3] Regardless of whether chlamydial antigens are presented by CD1d, the disruption of CD1d expression in *C. trachomatis*-infected cells may interfere with rapid and essential innate immune responses.

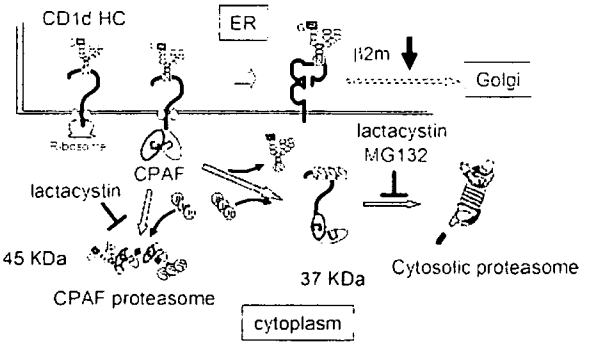

FIGURE 7. **Putative proteolytic degradation pathways for CD1d HCs upon *C. trachomatis* infection.** In *C. trachomatis*-infected cells, β2m-unassembled CD1d HC forms accumulate in the ER due to degradation of RFX5 by CPAF. CPAF secreted from the chlamydial inclusion into the cytosol interacts with the CD1d HC via cytoplasmic tail of the CD1d and CPAF is ubiquitinated. The binding of CPAF triggers dislocation of the 45-kDa immature glycosylated form of CD1d into the cytosol. One proteolytic pathway involves the conventional cellular proteasome. Glycosylated CD1d HC is ubiquitinated in the cytosol (ubiquitin ligase), and deglycosylated (peptide *N*-glycosidase) to create the 37-kDa non-glycosylated CD1d molecule. CPAF and the ubiquitinated, deglycosylated CD1d HC are degraded by the cytosolic proteasome. The alternative proteolytic pathway involves CPAF-mediated degradation. The 45-kDa immature glycosylated CD1d HC interacts with CPAF. CPAF targets the CD1d HC for degradation by a proteolytic activity distinct from that of the cytosolic proteasome. *Green symbols* indicated multiubiquitins.

Acknowledgments—We are grateful to Dr. G. Zhong for his kind gifts of anti-CPAF antibodies and purified CPAF c-fragment proteins, the Morphology and Imaging Core of the Louisiana State University Health Sciences Center Gene Therapy Program for facilitation of the fluorescent deconvolution microscopy, Dr. J. Nichols and J. Niles at University of Texas Medical Branch for facilitation of the flow cytometry studies, to C. D. McGahan and Dr. L. S. Graziadei for editorial assistance, and to Dr. Priscilla Wyrick for critical reading of the manuscript.

REFERENCES

1. Cates, W. Jr., and Wasserheit, J. N. (1991) *Am. J. Obstet. Gynecol.* 164, 1771–1781
2. Hogan, R. J., Mathews, S. A., Mukhopadhyay, S., Summersgill, J. T., and Timms, P. (2004) *Infect. Immun.* 72, 1843–1855
3. Beatty, W. L., Morrison, R. P., and Byrne, G. I. (1994) *Microbiol. Rev.* 58, 686–699

[3] K. Kawana and D. J. Schust, unpublished observation.

4. Zhong, G., Liu, L., Fan, T., Fan, P., and Ji, H. (2000) *J. Exp. Med.* **191,** 1525–1534
5. Zhong, G., Fan, T., and Liu, L. (1999) *J. Exp. Med.* **189,** 1931–1938
6. Zhong, G., Fan, P., Ji, H., Dong, F., and Huang, F. (2001) *J. Exp. Med.* **193,** 935–942
7. Dong, F., Pirbhai, M., Zhong, Y., and Zhong, G. (2004) *Mol. Microbiol.* **52,** 1487–1494
8. Bendelac, A., Lantz, O., Quimby, M. E., Yewdell, J. W., Bennink, J. R., and Brutkiewicz, R. R. (1995) *Science.* **268,** 863–865
9. Taniguchi, M., and Nakayama, T. (2000) *Semin. Immunol.* **12,** 543–550
10. Balk, S. P., Burke, S., Polischuk, J. E., Frantz, M. E., Yang, L., Porcelli, S., Colgan, S. P., and Blumberg, R. S. (1994) *Science* **265,** 259–262
11. Kim, H. S., Garcia, J., Exley, M., Johnson, K. W., Balk, S. P., and Blumberg, R. S. (1999) *J. Biol. Chem.* **274,** 9289–9295
12. Kang, S. J., and Cresswell, P. (2002) *J. Biol. Chem.* **277,** 44838–44844
13. Hirsch, C., Blom, D., and Ploegh, H. L. (2003) *EMBO J.* **22,** 1036–1046
14. Skold, M., and Behar, S. M. (2003) *Infect. Immun.* **71,** 5447–5455
15. Sanchez, D. J., Gumperz, J. E., and Ganem, D. (2005) *J. Clin. Invest.* **115,** 1369–1378
16. Brigl, M., Bry, L., Kent, S. C., Gumperz, J. E., and Brenner, M. B. (2003) *Nat. Immunol.* **4,** 1230–1237
17. Mattner, J., Debord, K. L., Ismail, N., Goff, R. D., Cantu, C., 3rd, Zhou, D., Saint-Mezard, P., Wang, V., Gao, Y., Yin, N., Hoebe, K., Schneewind, O., Walker, D., Beutler, B., Teyton, L., Savage, P. B., and Bendelac, A. (2005) *Nature* **434,** 525–529
18. Gumperz, J. E., Roy, C., Makowska, A., Lum, D., Sugita, M., Podrebarac, T., Koezuka, Y., Porcelli, S. A., Cardell, S., Brenner, M. B., and Behar, S. M. (2000) *Immunity* **12,** 211–221
19. Fichorova, R. N., Rheinwald, J. G., and Anderson, D. J. (1997) *Biol. Reprod.* **57,** 847–855
20. Cho, S., Knox, K. S., Kohli, L. M., He, J. J., Exley, M. A., Wilson, S. B., and Brutkiewicz, R. R. (2005) *Virology* **337,** 242–252
21. Yoshida, Y., Chiba, T., Tokunaga, F., Kawasaki, H., Iwai, K., Suzuki, T., Ito, Y., Matsuoka, K., Yoshida, M., Tanaka, K., and Tai, T. (2002) *Nature* **418,** 438–442
22. Yuan, W., Dasgupta, A., and Cresswell, P. (2006) *Nat. Immunol.* **7,** 835–842

Cyclic Regulation of T-Bet and GATA-3 in Human Endometrium

Danielle Inman, Kei Kawana, MD, Danny Schust, MD,
Ruth Lininger, MD, and Steven Young, MD, PhD

Endometrial cytokine expression is poorly understood. T-Bet and GATA-3 regulate cytokine expression in T-lymphocytes. Previous work has demonstrated expression of T-Bet in human endometrium. Changes in human endometrial T-Bet and GATA-3 mRNA and protein expression during the normal menstrual cycle were characterized. Human endometrium from each phase of the menstrual cycle underwent real-time reverse-transcriptase polymerase chain reaction and immunohistochemistry to examine expression and localization. T-Bet and GATA-3 mRNA were increased in the late secretory phase. Progesterone receptor (PR) mRNA was increased during the proliferative and early secretory phases. T-Bet and GATA-3 proteins localized cytoplasmically in the late secretory phase. PR protein displayed nuclear localization and maximal immunostaining during the early secretory phase. T-Bet and GATA-3 are expressed in endometrial epithelium cyclically during the menstrual cycle. T-Bet and GATA-3 are both upregulated during the late secretory phase and in the same cell types. The expression patterns of T-Bet and GATA-3 oppose PR, suggesting antagonistic function and/or regulation between PR and T-Bet/GATA-3.

KEY WORDS: T-Bet, GATA-3, progesterone receptor, human endometrium, reproductive immunology.

pithelial cells throughout the body function as a physical barrier to pathogen invasion. They also provide a chemical defense by recognizing and initiating immune responses to potential pathogens. Epithelial immune responses must be tightly regulated to prevent inappropriate immune responses to commensal or beneficial microbes. A major part of immune response by epithelia is the production and secretion of cytokines.

Endometrial epithelial cells are a rich source of cytokine production. Endometrial cytokines regulate local immune response but also act to regulate menstruation and embryo implantation. The regulation of cytokines in the endometrium is complex. This regulation must support immunological defense against pathogens, permit immunological tolerance to an invading semiallogeneic trophoblast, and enable the shedding and apoptosis that occurs during menstruation. However, the critical mechanisms regulating endometrial cytokine expression remain poorly understood.

In T-lymphocytes, 2 transcription factors—T-box expressed in T cell (T-Bet) and GATA-3—have a profound effect on the overall patterns of cytokine expression. For example, T-Bet is required for T cells to differentiate into a T_H1 cytokine expression pattern (interleukin [IL]–2, IL-3, interferon γ, and tumor necrosis factor–α).[1] In contrast, GATA-3 is required for T cells to differentiate into a T_H2 cytokine expression pattern (IL-4, IL-5, IL-6, IL-10, and IL-13).[2] The expression of T_H1 and T_H2 cytokines is usually mutually exclusive and generally thought to have opposing immunological function. It has been suggested that polarization of cytokine expression away from of the generally proinflammatory

From the Department of Obstetrics & Gynecology, University of North Carolina at Chapel Hill (DI, SY); School of Medicine, University of Tokyo, Japan (KK); Department of Obstetrics & Gynecology, University of Missouri (DS); and Department of Pathology, University of North Carolina at Chapel Hill (RL).

We gratefully acknowledge the financial support of the Holderness Foundation and the University of North Carolina Nova Carta Foundation. This research was also supported by the National Institute of Child Health and Human Development/National Institutes of Health through cooperative agreement U54 HD035041 as part of the Specialized Cooperative Centers Program in Reproduction and Infertility Research. We also gratefully acknowledge the outstanding technical assistance of Lingwen Yuan, PhD, Xi Yang, and Gail Grossman.

Address correspondence to: Danielle Inman, University of North Carolina at Chapel Hill, Department of OB/GYN, CB# 7570, 4001 Old Clinic Bldg Chapel Hill, NC 27599. E-mail: danielle_inman@med.unc.edu

Reproductive Sciences Vol. XX No. X Month XXXX xx-xx
DOI: 10.1177/1933719107309690

T_H1 response and toward the generally anti-inflammatory T_H2 response is essential for pregnancy maintenance and is altered in recurrent miscarriage.[3-12] Although there clearly is a bias toward T_H2 cytokine expression during pregnancy, the relative roles of eliminating T_H1 cytokine expression and promoting T_H2 response is debated.[3-12] Our recent finding of T-Bet expression in endometrial epithelium, a rich source of cytokine expression, suggests a possible role for T-Bet and GATA-3 in the regulation of endometrial cytokine expression and thus in pregnancy tolerance.[13]

Cytokines also play direct roles in the promotion of embryo implantation. For example, Stewart et al[14] showed that female mice lacking the expression of the cytokine leukemia inhibitory factor (LIF) are completely unreceptive to the implantation of embryos. As might be expected of a factor critical for implantation, endometrial epithelial LIF expression is cyclic and regulated by reproductive steroid hormones.[15] We recently demonstrated reproductive hormone regulation of T-Bet expression,[13] echoing an earlier study showing effects of low-dose estrogen on T-Bet expression and/or activity in the brain.[16] In vitro evidence also supports estradiol upregulation of GATA-3 and downregulation of T-Bet mRNA.[17] We hypothesized that estrogen and progesterone regulation of T-Bet and GATA-3 would in turn regulate local cytokine expression, resulting in changes in endometrial function. We also hypothesized that T-Bet and GATA-3 would be subject to opposing cyclic regulation since expression of each directly inhibits expression of the other in T lymphocytes.[18] Thus, we sought to characterize endometrial T-Bet and GATA-3 RNA and protein expression in each phase of the normal menstrual cycle using quantitative reverse-transcriptase polymerase chain reaction (qRT-PCR) and immunohistochemistry.

METHODS

Endometrial Specimen Collection and Preservation

Endometrial specimens were collected from healthy volunteers under a protocol approved by the Institutional Review Board of the University of North Carolina at Chapel Hill. All women were between 19 and 34 years of age and were not taking any medications that are known to affect reproductive hormone production or action. Endometrial sampling was done using a Pipelle sampler. Samples were divided into portions and flash frozen in liquid N_2 or placed in formalin. The formalin-fixed samples were embedded in paraffin and sectioned for immunohistochemistry and staining with hematoxylin and eosin (H&E). The flash-frozen samples were used to generate RNA for real-time RT-PCR.

Cycle Day Identification

Two methods were used to determine the secretory phase day of each sample. Prior to biopsy, urinary luteinizing hormone (LH) surges were monitored by the subjects using home test kits. Postbiopsy, H&E-stained sample morphologies were blindly analyzed by a pathologist using microscopy.

RNA Isolation and Quantification

Endometrial total RNA was isolated from 21 frozen tissue samples using the RNAqueous-4PCR Kit (Ambion, Foster City, CA) and the manufacturer's suggested conditions. RNA was quantitated using RiboGreen (Molecular Probes, Carlsbad, CA) with a ribosomal RNA standard curve. First-strand cDNA was synthesized from 100 ng of total RNA using the Roche 1st Strand cDNA Synthesis Kit for RT-PCR.

For T-Bet, each sample of cDNA was diluted 1:25 and plated in triplicate. Detection used the following primers and probe (Synthegen, Houston, TX): forward primer, 5′-AAGTTTA ATCAGCACCAGACAGAG-3′; reverse primer, 5′-GCCACAGTAAATGACAGGAATGG-3′; and probe, 5′-AACATCCGCCGTCCCTGCTTGGTG-3′. Primers and probes for cyclophilin (PPIA), progesterone receptor, and GATA-3 were obtained in a predesigned mix for each gene (Gene Expression Assays; Applied Biosystems, Foster City, CA). The efficiency of each primer probe set was run on each analysis day and used serial dilutions of peripheral blood mononuclear cell cDNA. The total reaction volume for all real-time PCR experiments was 25 µL. All reactions were performed in 96-well plates on a Stratagene MX3000 device for 40 two-step cycles (95°C for 20 seconds and then 60°C for 1 minute) and used a commercially prepared master mix (ABI).

The efficiency of all PCR reactions ranged from 97% to 103%. The average cycle number at which the TaqMan fluorescence became detectable above the threshold (Ct) was 31.4 (T-Bet), 27.8 (GATA-3), 23.0 (progesterone receptor [PR]), and 19.6 (PPIA). Ct values were converted to

relative expression using the ΔΔCt method, allowing normalization to both the housekeeping gene, cyclophilin (PPIA), and a single sample in the early secretory phase (LH2) for T-Bet, GATA-3, and the late secretory phase for PR.

Tissue Preparation and Immunolocalization

Paraffin-embedded tissue samples (n = 8) were sectioned and mounted onto slides. Duplicate samples were subjected to antigen retrieval using boiling (100°C) citrate buffer (pH = 6.0) for two 5-minutes intervals. Following antigen retrieval, the slides were immersed in 0.3% H_2O_2 + methanol for 30 minutes to quench endogenous peroxidase activity. The T-Bet antibody (4B10-sc21749; Santa Cruz Biotechnology, Santa Cruz, CA), GATA-3 antibody (MAB260501, clone-291106; R&D Systems, Minneapolis, MN), PR antibody (A/B,VP-p977;Vector Laboratories, Burlingame, CA), ER (positive control) antibody (NCL-ER-6F11; Novocastra, Norwell, MA), and IgG isotype (negative control) antibody (MAB002; R&D Systems) were diluted 1:20, 1:200, 1:50, 1:40, and 1:50, respectively. The sections were incubated with primary antibodies overnight at 4°C. The secondary antibody, biotinylated goat antimouse IgG (BA-9200;Vector Laboratories) was diluted 1:100 and incubated for 1 hour at room temperature. The stain was then developed using an ABC kit (Vector Laboratories). The slides were rinsed and counterstained with 5% hematoxylin (DAKO, Glostrup, Denmark).

RESULTS

Healthy, regularly menstruating volunteers had an endometrial biopsy timed by daily urinary LH surge measurements. An aliquot was placed in formalin for later immunohistochemistry, and the remaining tissue was flash frozen in liquid nitrogen. RNA was extracted from frozen tissue, and relative expression of T-Bet and GATA-3 mRNA at each phase of the menstrual cycle was determined using real-time RT-PCR. The analysis of mRNA expression was based on 3 proliferative samples (cycle days 1-14), 6 early secretory samples (post LH surge days 1-4), 9 midsecretory samples (post–LH surge days 5-9), and 3 late secretory samples (post–LH surge days 10-14). The relative expression of PR, which is expected to fall

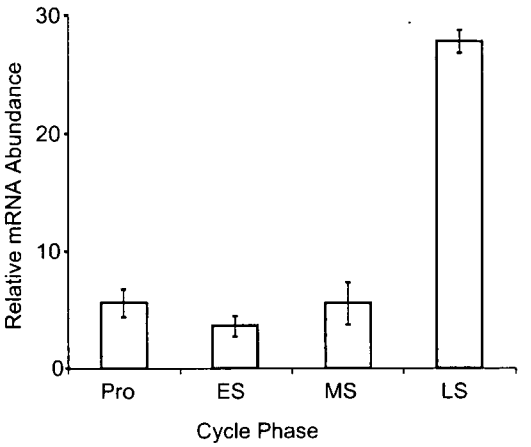

Figure 1. Relative expression of T-Bet mRNA across the menstrual cycle. Relative mRNA expression was calculated after real-time reverse-transcriptase polymerase chain reaction using the ΔΔCt method, with cyclophilin as a housekeeping control gene. Data are expressed as the mean ± standard deviation of samples grouped by menstrual cycle phase. *$P < .01$ as compared with all other phases using 1-way analysis of variance with the Tukey post hoc test. Pro indicates proliferative; ES, early secretory; MS, midsecretory; LS, late secretory.

in the mid and late secretory phases,[19] was used as a control. Cyclophilin (PPIA) was chosen as a housekeeping control gene because it varied only minimally in this sample set and in other endometrial sample sets in our experience (data not shown).

Formalin-fixed sections were stained with H&E, and histological dating was performed using the criteria of Noyes et al.[20] LH surge and histological dating showed the same trends. However, if the sample was within 1 day of being in a different cycle phase, histological determination was used to allow reassignment to 1 day later or earlier and thus to the other cycle phase.

A 25-fold increase in T-Bet ($P < .01$; Figure 1) and a 6-fold increase in GATA-3 ($P < .01$; Figure 2) were observed during the late secretory as compared with the early secretory phase. The same samples demonstrated a 30-fold decrease in PR between the early and late secretory phases (Figure 3). Thus, a specific upregulation of mRNA for both T-Bet and GATA-3 is seen (Figures 1-3).

After identifying the changes in mRNA levels in whole endometrial tissue, we next sought to identify the cell types expressing T-Bet and GATA-3 protein and whether relative protein expression was predicted by mRNA levels. Immunohistochemical localization of T-Bet, GATA-3, and PR was evaluated at each phase of the menstrual